Dear Editors, dear reviewers,

Many thanks for the comments on the paper. I have addressed everything to my best abilities and think that the paper has improved because of it. I hope there are no further queries.

Below, I reply to the reviewers' comments in detail, given first their comment, then my reply in *italics*.

With best wishes, Jens Turowski

Summary of changes

- I removed previous figure 5. The calculations shown there were unrealistic and only of technical interest. Since they seem to have confused Reviewer #3, I have decided to remove them from the paper. This does not affect the central argument.
- I have added a paragraph in the discussion (section 4.1), discussing potential limits of the model assumptions. In particular, the issue of the bar wavelength and scaling is discussed in some detail.
- I have gone through the text, trying to improve flow, clarity and readability.

Reviewer #1

In this manuscript, the author proposed a mechanistic model for analyzing the adjustment timescales for channel width, channel bed slope and alluvial bed cover in a mixed alluvial - bedrock channel. However, in the current version a significant question on the assumption of the bar wavelength remains and needs to be addressed.

In eq. 23, you assumed that the bar wavelength decreases with decreasing the fraction of alluvial cover. However, recent studies indicate that the bar wavelength increases with decreasing the fraction of alluvial cover in mixed alluvial – bedrock channel, in theoretically (Nelson and Seminara, 2011, Fig.2b, doi: 10.1029/2011GL050806) and numerically (Inoue et al., 2016, Figs 5 and 11, doi: 10.1061/(ASCE)HY.1943-7900.0001124.). Experiments conducted by Chatanantavet and Parker (2008) also show no decrease in bar wavelength. Your assumption is based on Kelly (2006)'s observations in alluvial channel, but may not be applicable to mixed alluvial – bedrock channel. Because this assumption directly affects the lateral erosion rate and the timescales, the results shown in Figs 4 – 6 may be incorrect.

I acknowledge that the assumption I have made is based on data for alluvial streams. I made this assumption because there is little (no) relevant data available for bedrock channels. This was stated in the original manuscript. The reviewer disputes this statement, citing three articles for support, two modelling papers (Nelson and Seminar, 2011, which was likely confused with Nelson and Seminara, 2012; Inoue et al., 2016) and one experimental paper (Chatanantavet and Parker, 2008). As I have already stated in my initial reply in the discussion forum, I was not able to find this evidence in the mentioned papers. In his reply to my comment in the forum, the reviewer mentions another paper by Chatanantavet and Parker, 2018. Below, I will comment on all of these papers, and elaborate my point of view on this in a little more detail.

First, none of the mentioned papers was set up to investigate the problem of bar length, bar geometry and bar wavelength. The reviewer has not been able to point out explicit relevant *statements on the matter within the mentioned papers, and instead cites various figures, especially from the experimental paper, in support.*

Nelson and Seminara, 2011: This paper deals with channel cross-sectional shape and does not mention bars.

Nelson and Seminara, 2012: Here, the authors investigate initial bar instability, not bar geometry. They explicitly state that their analysis is not suitable for making statements about the emerging forms (paragraph 25): "It is important to emphasize that the linear analysis presented here only addresses the initial instability which generates bar like patterns. Predicting the actual pattern emerging from this process will require a fully nonlinear analysis possibly able to treat regions where the areal sediment concentration C locally reaches 1 and local alluviation occurs." It would be the latter (steady state bar geometry) that is relevant for my model. Concluding, the Nelson and Seminara 2012 paper does not contain statements relevant for the debate.

Inoue et al., 2016: The authors use a numerical model to study the transient adjustment of cover and bedforms, keeping boundary conditions constant. For this paper, the reviewer refers to Figures 5 and 11 in his argument. Figure 5 shows 6 maps at consecutive times, and indeed, here it looks like bar wavelength is constant as deposition continues. Figure 11 shows three similar time slices. Alternating bars appear in the third (last; 500 hours) shown slice, and a comparison of bar wavelength for different slices is thus not possible. If the deposition in time slice 2 (250 hours) is interpreted to show alternating bars, the wavelength seems to be longer, of the order of the length of the experimental reach. In this interpretation, Figure 7 would suggest an evolution of bar wavelength over the course of the experiment. There is another relevant figure in the paper, Figure 14, which shows three time slices of a simulations set to correspond to conditions studied by Chatanantavet and Parker, 2009, in experiments. These can also be interpreted to show bar wavelength that is not changing over the course of the experiment. There is a fundamental difference between the model conditions studied in this paper and the assumptions I make for my model set up: While Inoue et al. study transient adjustment to a steady state cover, starting from an empty bed, all applications within my paper build on the assumption of steady state cover (eq. 32; see also Turowski and Hodge, 2017). A comparison also needs to take into account this aspect.

Regarding both modelling papers (Nelson and Seminara, 2012; Inoue et al., 2016), I would like to also repeat the statements from Inoue et al., that I quoted in my comment in the forum (page 8, left-hand column, 2nd full paragraph): "Nelson and Seminara (2012) conducted a linear stability analysis of bars on the bedrock and analyzed the wavelength of infinitesimal bars. The findings of their analysis are as follows: (1) regions where alternate bars form on the bedrock are determined not only by the width/depth ratio, but to some degree by the ratio of $\tau = \tau c$; and (2) the wavelength of the bars increases with decreasing sediment supply rate. The analysis by Nelson and Seminara (2012), unlike the simulation of this study, did not consider localized bedrock erosion by bedload; therefore, it is not possible to compare the two simulations quantitatively. However, the two models show a similar tendency to form longer wavelength bars when the sediment supply is lower." I read this to support my assumption. In his/her reply to the comment, the reviewer did not explicitly address this quote. She/he did state, however, that "You may be confusing the length of an individual bar patch with the length between two bar patches". This may be the case, but given the sparsity of information it seems to be the most straightforward interpretation of the above statement.

Chatanantavet and Parker, 2008: The authors use flume experiments to investigate how cover changes with sediment supply (or rather, the ratio between supply and transport capacity) for various conditions and bed topographies. They mention that alternating bars were present in the *experiments (e.g., paragraph 13), but do not give details on their morphology or how their wavelength scales with cover. Figure 11 seems to be the only figure containing relevant material. The question of bar wavelength is difficult to assess from this figure: picture quality is low because of water surface reflections, there is a single wavelength within the shown part of the flume, and it is unclear whether this shows a transient or steady state. As evidence, this is at best suggestive or circumstantial. Reviewer #3 agrees on this assessment and states explicitly that she/he interprets this figure to support my assumption, rather than the claim of reviewer #1. I hesitate to make a final judgement on such thin evidence.*

Chatanantavet and Parker, 2018: I was not able to find this paper. Please supply a full reference.

In summary, the evidence presented in the three mentioned papers is at most suggestive. There is an additional complication. Even if I was convinced that bar wavelength is independent of cover, bar wavelength needs to depend on something. It seems safe to me to state that we currently do not understand the geometry of alternating bars in bedrock channels and what controls it. Simple dimensional analysis suggests that at least one other length scale is required. I chose bar width for this length scale, keeping the aspect ratio constant. As long as we do not have full understanding of the controls, another assumption needs to be made (for example, a dependence on channel width or flow depth), for which there is little evidence either. In light of the currently available evidence, my strategy of using an alluvial analogue seems to me still the best and most plausible option. I would be very happy to change this approach if convincing evidence is supplied.

All this said, I repeat my statement from the reply comment in the forum: A change in the bar geometry affects only the lateral erosion equation (eq. 24 in the paper). This propagates into the response time of width for a widening channel, but not the response time of cover, of bed slope or for the width for a narrowing channel. The response times for widening will be substantially affected only when the bar aspect ratio deviates substantially from the value of 2-10 that I assumed (5 for the example calculations). This is likely the case only for low values of bed cover. Changing the assumption on bar geometry does not affect the steady state channel morphology presented in Fig. 4. In summary, a change in the dependence of bar wavelength on cover would not change the arguments and conclusions of the paper. The issue of bar wavelength is a minor part in the argument of the paper and does not change the overall conclusions, the narrative and the general points that I am trying to make. As a result, I find the overall negative assessment of the paper, based on this single minor criticism, to be unjustified.

In response to the reviewer's comment, I added a paragraph in the discussion on the bar geometry issue. I also point out the caveat mentioned in the forum comment that due to the constant aspect ratio, bar wavelength approaches zero as cover approaches zero. This seems to be unphysical and needs to be addressed in a fully dynamic model. I also stress that for all the calculations presented in this paper, the assumption of steady state cover is made.

Additional comments by line number below:
P2 Eq. (1): The density of the sediment?
Changed.
P7 Line 9: Auel et al., 2017 a or b?
2017a, corrected.
P7 Line 15: Why does the secondary flow not affect the lateral impact velocity?
It probably does, but we have few constraints on it. The available data suggest that roughness is the most important control. See the discussion in Turowski, 2018.

P7 Line 32: Nelson and Seminara analyzed alternate bars in a mixed alluvial – bedrock channel in 2012, not 2011. The paper listed in the reference is probably incorrect.
Corrected.
P12 Figure 4c: There is no explanation of Fig4c in the text. Why does slope and width change with uplift rate?
The assumption here was that incision rate is equal to uplift rate in steady state.
P15. Line 6: Gravel bars do not increase their wavelength as cover increases.
See discussion above on the major point.
P19 Eq. (B6): When C is close to 0 (i.e., almost completely exposed bedrock), is close to 90 degree (i.e., sediments move towards the sidewalls). Why?
This is due to the coupling of bar wavelength to cover – the amplitude of the sine wave is small in comparison to the channel width, making the angle very steep. This seems unphysical. I have added a paragraph in the discussion.
P26-P29: Inoue et al. (2014), Montgomery et al. (1996), Shepherd (1972) and Whipple (2004) are not listed in the references.
Missing references added.

Reviewer #3

In this paper, the author investigated the adjustment timescales of width, slope, and bed cover for bedrock rivers, via theoretical framework and numerical computations. I think the idea is significant and interesting, especially he included the lateral erosion. The English is very good. I just have some comments below, one of which may affect the orders of magnitude of adjustment timescale, however. So please consider.

Seeing the exchanges between the anonymous reviewer #1 and the author, I went back and checked the paper by Chatanantavet and Parker 2008. In their figure 11 (especially comparing the subfigures 2 and 4), at first glance I thought the assumption by the author Turowski was correct, i.e. the bar wavelength decreases with decreasing fraction of alluvial cover. But I could be wrong since I have not done any direct research regarding alternate bars or meandering channels. In the last interactive comment, the anonymous reviewer #1 stated that “although the bar patch length has a positive correlation with both the bar width and the alluvial cover, the wavelength has no positive correlation.” It is hard to assess quantitatively and would need a longer flume length. I leave it to the AE and the editor to digest.

Major comments:
- I really think you should include a factor of “flood intermittency” (a fraction of time duration in a year that has water discharge significant enough to do the majority of bedrock abrasion). This is commonly done in any morphodynamical modeling of such a temporal process involving high flow: see any papers done by the research groups of Chris Paola and Gary Parker (e.g., Chatanantavet and Parker 2009). For example, your Exner equation (eq.4 and then eq. 28, 34) does not have this factor and go on to derive the timescale for slope adjustment (eq 37). Say, if flood intermittency is equal to 0.05-0.1 in a particular location. Then your slope adjustment timescale could be missed by a factor of 10-20. That is significant and may affect your conclusion. I think it would make the adjustment timescale longer. In table 1, for example, you wouldn’t expect that water discharge of 40 m3/s is present for the entire year in the Liwu river.
This is an excellent point. The representative discharge I used for the calculation is actually a representative discharge of all flows that transport bedload and could therefore contribute to erosion. The method for the discharge partitioning was developed by Sklar and Dietrich (2006). This is described in

the Turowski et al. (2007) paper, from which the numbers originate, but was not explained in the present manuscript. I have now added this explanation. As such, flood intermittency has been taken into account in an implicit way.

- The part where you talk about lateral erosion and alternate bars (i.e. section 2.2 and elsewhere); I think that it is worth or even very important to note to the readers that these morphological configurations occur only in a specific range of channel slope in natural setting, which is around S = about 0.1-3% per Montgomery and Buffington 1997, and other studies. Beyond this slope range, i.e. at S = 3% or higher until S = about 10%, steep-pool configuration dominates bedrock channels and its associated sediment transport differ quite significantly since there is strong coupling interaction between hydraulic jump hydrodynamics and sediment trajectory/movement (see any flume experimental work in step pool). Hence, in your paper when you talk about lateral erosion and alternate bars, the conceptual model may be limited to slope of no more than 2-3% (or 0.02-0.03). Seeing that slope in your results span until 0.1 (figure 5D), it is a bit farfetched. This slope cutoff is eminent whenever I conducted flume experiments ranging slope from 0.1% to 5%; once the slope hit 3% the step pools were very obvious and the hydraulics and associated sediment transport were so much different from alternate bars (or pool riffle) or plane-bed feature.
Excellent point. I have added a paragraph on the limits of model assumptions to the discussion in 4.1, mentioning this and some other points. I left the presentation of results as is for the interest of the reader. Model assumptions are clearly laid out and there should hopefully be no confusion for a careful reader.

- P12 L5; critical Shields stress also varies with channel slope (e.g., Lamb et al, 2008, JGR-ES; Chatanantavet et al. 2013, JGR ES). I know traditionally and simplistically people assume that it is constant, but it is an old concept. And this can affect your numerical results greatly because unlike alluvial rivers, bedrock rivers has varying slopes in a high value range (around 0.001-0.1, in which alluvial rivers don't touch but odd things happen here such as hydraulic jumps).
I am of course aware of this. I have consciously decided not to use the Lamb equation – first, it is unphysical in the limit of low slopes, where the value should stabilize around a classical value of 0.045 or so. There is also a temporal dependence complicating the picture (see for example recent work of Claire Masteller). And the explicit dependence of slope would add yet another feedback to already complicated equations. There are also field data, refuting the simple trends described by the Lamb equation (see for example publications by Kristin Bunte). In the end, the addition would not majorly change trends, it would not yield any further interesting insights, and would not change the main argument and message of the paper.

- Page 10; the response time ratios. Sorry, I don't get why you wrote up this section. I don't see its usefulness and you didn't explain why this needs to be done. You also did not use any of these to plot the results or discuss about it.
The response time ratios are plotted in Figures 5 b, d, and f (previously Fig. 6). The argument put forward in section 4.3 is based on these calculations. I added a couple explanatory sentences to the start of section 2.3.4.

- There is a paper by Sklar and Dietrich 2006 (Geomorphology) titled "The role of sediment in controlling steady-state bedrock channel slope: Implications of the saltation–abrasion incision model". I think it is worth to check it out if you have not already. Actually their work is highly related to yours, along the same concept (i.e. their figure 6 vs your figure 4) and should be acknowledged. I understand that your work added lateral erosion and so on, which is cool. Actually looking at their figure 6, it reminds me that sensitivity analysis should be implemented with this kind of studies.

I am aware of this paper, but had not read it for some time. I do not want to give a full criticism of this paper here, but I think the linear decomposition (their eq. 32) is incorrect, and for this reason their results are fundamentally flawed.

I am not quite sure what the reviewer is asking for here. The equivalent to their Fig. 6 is my Fig. 4c. A cross-comparison of different model approaches is beyond the scope of my paper, and in my mind not particularly useful, because sufficient data for a clean discrimination are currently lacking. In any case, I have already demonstrated in a previous paper (Turowski ESurf 2018) that the model predictions for steady state are in agreement with all currently available data on the reach scale, because it predicts the observed scalings of width and sinuosity in addition to that of slope. This is in contrast to any other models I know of. With regard to steady state geometry, the novelty of the present paper is the quantification of the sideward deflection length scale d. Figure 4 demonstrates that this quantification does not change the analysis made in the previous paper. This point is made and discussed in section 4.2, where I have now added a sentence to make this clearer.

In the revised manuscript, the Sklar and Dietrich 2006 paper is now cited because it describes a discharge partitioning method used to obtain the representative discharge for the Liwu (Table 1).

- If I understand correctly, your results in figures 4, 5, 6 are dealing with specific boundary conditions at any specific point/reach section in a channel. But I am afraid, as the figures stand now, the presentation might mislead some readers to think that slope and channel width (and cover) are spatially constant along a whole bedrock channel length. As you know, both slope and channel width are not spatially constant along bedrock channels. And we often see concave or convex or straight bedrock streams. When investigating steady state conditions of river channels, I think it would be cool to see plots of spatially distributed features of the variables in questions. OR at least discuss about it, or even mathematically. This is especially when you show “reach length” of 10 km in Table 1. So the readers may visualize and think you are talking about the whole channel length. I feel like the work is incomplete by having no spatially distributed results or talking/discussing about it. You have great math framework already and some initial results in figs 4-6. Having these additional figures would enhance the paper nicely (in that case, you might need to add some equations to implement).

I do not fully understand this comment.

In Figure 4, I show steady state slope and width as a function of forcing parameters (uplift rate, water discharge, sediment supply). Here, the dependence on slope and width can be explicitly seen – and they are mostly not constant! Note for example the concavity of the channel in Fig. 4a – the decline only looks linear because of the log-log scale. The interesting exception is that width is predicted to be explicitly independent of water discharge. This is surprising because we all know about the typical scaling W~sqrt(Q). This scaling arises in the model from the covariance of water and sediment discharge. The point is discussed in some detail in section 4.2. See also the discussion in Turowski, ESurf 2018.

Figures 5 and 6 show response time scales, rather than channel geometry. For Figure 5, I used the values from Table 1, for Figure 6, slope, width and cover were calculated according to the model. I do not see how these could give the impression of constant slope, width, or cover. The value of the reach length is needed for these calculations, because slope is adjusted by knickpoints migration, which needs to move through the entire reach for a full adjustment. Similarly for the adjustment of cover: for a given supply

rate, adjustment times obviously are dependent on the amount of area that needs to be covered, which is set by the product of length and width.
A reach is defined as a stretch of the river over which boundary conditions and, as a consequence, channel geometry is roughly constant. So it should not come as a surprise that width and slope are constant within a reach.
*The reviewer asks for a plot of 'spatially distributed features'. I understand this as a plot against river length or some kind of other distance. But, in essence, the plot against discharge (Fig. 4a) is doing exactly that. River length is not a control variable. To produce such a plot, I would need to make an assumption about how discharge scales with drainage area (hydrology, for example Q~P*A, where P is the precipitation rate), and then an assumption about how drainage area scales with length (basin geometry, for example Hack's law). These assumptions may apply in some regions but not in others. Plotting against discharge is more natural, as it keeps the relationship between forcing and response explicit and direct. I do not think such a plot would be useful and have not included one.*
In summary, I think that Fig. 4 is essentially supplying the information that the reviewer is asking for. There seems to be some misunderstanding about the contents of Fig. 5 and 6, but I am unsure about what that is exactly.
I have tried to improve the clarity of the text. I have also removed Fig. 5 to avoid confusion. The information in this figure was mainly of technical interest and can be easily reproduced with the information given in the paper.

Minor comments
P1, L9; an alluvial (use lower case after colon)
Changed.
P1, L11, 14; "…a balance between channel incision and uplift" sounds better, I think.
Changed.
P1, L13; I think "in the present work" sounds more formal and commonly used than "within the present paper"
Changed.
P1, L19; if these are from your results, please indicate clearly by saying "My results show that …" or something like that.
P1 L29; various timescales
Corrected.
P1 L35; delete "for"
Changed to 'in'.
P1 L38; is temporally constant
I prefer the current phrasing. No changes.
P3 L6-L18; in this paragraph, I think you should explicitly state somewhere that you only investigate the bedrock incision process due to bedload abrasion, and NOT consider plucking, suspended abrasion, etc. Also in discussion section, you don't touch this topic.
This is a good point; however, this is not the right paragraph, because mechanisms of erosion have not been introduced here. I added a statement at the beginning of section 2.
P3 L1-L4; you may want to add a reference here such as Chatanantavet and Parker 2009 and/or a few other studies who used this equation to show how bedrock rivers approach a steady state. Readers who wish to read further in details can see how steady state profiles look like for bedrock channels.
The shape of a bedrock channel long profile depends on the assumptions of the erosion mechanisms, and its mathematical description. Eq. 1 has been used in many studies – most current landscape evolution models use it as a basic mass balance equation, it is also used for stream-profile inversion using the

stream power model. I think citations to particular modelling studies would be misleading here. I could not find many papers explicitly stating the equation – for example, the early Whipple and Tucker papers always give the stream power model first and then state 'combined with a statement of conservation of mass' or similar. I have added a citation of Howard 1994, who explicitly stated the equation.

P3 L23; this sentence is quite awkward. Consider reword.

Moved 'third' to the start of the sentence.

P5; you have here 2.2.1 but then 2.3 . I think probably you better just delete sub-section 2.2.1 and merge the text with 2.2.

Removed the sub-heading to 2.2.1.

P10 L15-16; the font size here is different.

Changed.

Mass balance, grade, and adjustment timescales in bedrock channels

Jens Martin Turowski[1]

[1] Helmholtzzentrum Potsdam, German Research Centre for Geosciences GFZ, Telegrafenberg, 14473 Potsdam, Germany

Correspondence to: Jens M. Turowski (turowski@gfz-potsdam.de)

Abstract

Rivers are dynamical systems that are thought to evolve towards a steady state configuration. Then, geomorphic parameters, such as channel width and slope, are constant over time. In the mathematical description of the system, the steady state corresponds to a fixed point in the dynamic equations in which all time derivatives are equal to zero. In alluvial rivers, steady state is characterised by grade. This can be expressed as a so-called order principle: ~~An~~ an alluvial river evolves to achieve a state in which sediment transport is constant along the river channel, and is equal to transport capacity everywhere. In bedrock rivers, steady state is thought to be achieved with a balance between ~~erosion~~ channel incision and uplift. The corresponding order principle is: A bedrock river evolves to achieve a vertical bedrock incision rate that is equal to the uplift rate or baselevel lowering rate. ~~Within~~ In the present ~~paper~~work, considerations of process physics and of the mass balance of a bedrock channel are used to argue that bedrock rivers evolve to achieve both grade and a balance between ~~erosion~~ channel incision and uplift. As such, bedrock channels are governed by two order principles. As a consequence, the recognition of a steady state with respect to one of them does not necessarily imply an overall steady state. For further discussion of the bedrock channel evolution towards a steady state, expressions for adjustment timescales are sought. For this, a mechanistic model for lateral erosion of bedrock channels is developed, which allows to obtain analytical solutions for the adjustment timescales for the morphological variables of channel width, channel bed slope and alluvial bed cover. The adjustment timescale to achieve steady cover is of the order of minutes to days, while the adjustment timescales for width and slope are of the order of thousands of years. Thus, cover is adjusted quickly in response to a change in boundary conditions to achieve a graded state. The resulting change in vertical and lateral incision rates triggers a slow adjustment of width and slope, which in turn affects bed cover. As a result of these feedbacks, it can be expected that a bedrock channel is close to a graded state most of the time, even when it is transiently adjusting its bedrock channel morphology.

1 Introduction

Bedrock rivers are important geomorphic landforms in mountain regions. They set the baselevel for hillslope response and evacuate the products produced by erosion, weathering and hillslope mass wasting (e.g., Hovius and Stark, 2006). As such, they integrate the upstream erosional signal of the landscape, and the material transported in rivers can be used to estimate catchment-averaged denudation rates on ~~varies~~ various timescales (e.g., Turowski and Cook, 2017). Further, their morphology is thought to be indicative of past climate and tectonic conditions (e.g., Stark et al., 2010; Wobus et al., 2006). Consequently, they provide archives that can be exploited to unravel the Earth's history.

River channels are dynamical systems. Their state variables – for example, slope, cross-sectional shape, and bed roughness – evolve over time under the influence of externally imposed driving variables including water discharge, sediment supply, and tectonic uplift (e.g., Heimann et al., 2015; Lague, 2010; Parker, 1979; Wickert and Schildgen, 2019). Like ~~for~~ in many other dynamical systems, there exists a fixed point in the descriptions of river dynamics, at which all state variables are constant over time. In an alluvial river, at this fixed point, entrainment and deposition of sediment are in balance along the river profile, implying that sediment transport rate is constant and that sediment transport capacity matches sediment supply. A river that exhibits these features is said to be 'in grade' or 'graded', because it is neither aggrading nor degrading (Mackin, 1948). Since its introduction, the graded stream concept has become a central paradigm in river morphodynamics (e.g., Blom et al., 2017; Church, 2006). There are several reasons for this importance. Chiefly, rivers are physically complicated systems, and the description of their steady state forms is a problem that is considerably simpler than the full description of their dynamics. Further, many variables of natural rivers are challenging to measure. Yet, comparatively simple scaling relations have been observed between variables such as ~~the~~ discharge or drainage area, on the one hand, and channel width ~~and~~ or channel slope, on the other hand (e.g., Gleason, 2015; Leopold and Maddock, 1953; Whitbread et al., 2015). ~~which~~ These scaling relationships are thought to be explainable using steady state models (e.g., Eaton and Church, 2004; ~~Leopold and Maddock, 1953;~~ Smith, 1974; Turowski, 2018; Wobus et al., 2006).

The condition of grade in a stream is tightly connected to the description of its sediment mass balance. For alluvial rivers, this mass balance is typically described by one of two approaches, the Exner equation or the entrainment-deposition framework (e.g., An et al., 2018). In the Exner equation (e.g., Chen et al., 2014; Paola and Voller, 2005), the rate of change of the sediment bed elevation h_s is related to the long-stream divergence of sediment supply per unit width, q_s.

$$\frac{\partial h_s}{\partial t} = -\frac{1}{\rho_{\cancel{r}s}(1-p)}\frac{\partial q_s}{\partial x}$$

(1)

Here, p is the porosity and ρ_r the density of the ~~rock~~sediment, t the time and x the distance in the downstream direction. In steady state, for a graded stream, the time derivative on the left-hand side is zero, which implies that the spatial derivative on the right-hand side is zero also. As a result, the sediment flux is constant along the stream – the stream is in grade. Any bed elevation change leads to an adjustment of slope. The condition of grade thus implies that transport capacity is also constant and equal to sediment supply along the stream. In the entrainment-deposition framework (e.g., Charru et al., 2004; Davy and Lague, 2009; Shobe et al., 2017), the entrainment rate E and deposition rate D of sediment mass per unit area are tracked explicitly, giving the mass balance for the mobile sediment mass per unit area M_m (e.g., Turowski and Hodge, 2017)

$$\frac{\partial M_m}{\partial t} = -\frac{\partial q_s}{\partial x} + E - D$$

(2)

The sediment bed elevation change is then described by a second equation

$$\frac{\partial h_s}{\partial t} = \frac{1}{\rho_{\cancel{r}s}(1-p)}(D-E)$$

(3)

Within this framework, in steady state, time derivatives are set to zero, implying that entrainment needs to equal deposition (eq. 3) and sediment flux along the stream needs to be constant (eq. 2). Again, this means that the stream is in grade. The main advantage of the erosion-deposition framework is that it keeps separately track of stationary and moving sediment mass. This is allows to predict a lagged response of bed elevation to changes in sediment supply, due to the interplay of entrainment, deposition and lateral sediment movement (e.g., An et al., 2018). Its main disadvantage is that both entrainment and deposition (E and D in eq. 2 and 3) need to be quantified in terms of hydraulic drivers. In contrast, to use the Exner equation, only transport capacity or transport rate needs to be quantified, which is considerably easier to measure than deposition and entrainment rate, and therefore the relevant relationships are better constrained. Nevertheless, both approaches are related and the entrainment-deposition equations (2 and 3) can be transformed into the Exner equation (1) when combining mobile and stationary mass into a single total mass term (Appendix A).

In bedrock channels, the concept of grade has not been widely applied. One of the main reasons for this is that bedrock channels are usually viewed as detachment-limited systems, where sediment supply is much smaller than transport capacity (e.g., Tinkler and Wohl, 1998; Whipple et al., 2013), which is in direct contrast to the assumption of grade. As a result, the system is assumed to be driven by its potency for erosion (e.g., Whipple, 2004). The evolution of bedrock channel bed elevation h_b is described by the equation (e.g., Howard, 1994)

$$\frac{\partial h_b}{\partial t} = T_U - I \tag{4}$$

Here, T_U is the uplift rate or relative baselevel fall rate and I the bedrock incision rate. According to equation (4), bedrock channels adjust to a steady state in which incision rate I equals uplift rate T_U.

Over the last two decades, evidence has been mounting that fluvial bedrock erosion is driven by the impacts of sediment particles in many settings (e.g., Cook et al., 2013; Johnson et al., 2010; Sklar and Dietrich, 2004). The amount of sediment in the channel affects erosion rates by two main effects. First, an increase in the number of moving particles leads to an increase in the number of impacts on the bed, increasing erosion rates. This is known as the tools effect. Second, sediment residing on the bed may protect the rock surface from impacts, reducing erosion rates. This is known as the cover effect. Evidence for both tools and cover effects have been described in laboratory and field studies (e.g., Beer et al., 2016; Cook et al., 2013; Johnson and Whipple, 2010; Sklar and Dietrich, 2001; Turowski et al., 2008a). In addition, large sediment bodies can reside in mountain areas in and around stream channels for potentially long time (e.g., Korup et al., 2006; Schoch et al., 2018). All of these observations imply that a description of the mass balance of sediment should be an essential part of any theoretical description of bedrock channels. In addition, recent observations have been interpreted such that bedrock channels are in a graded state, similar to alluvial channels (Phillips and Jerolmack, 2016). Thus, it seems that the view that bedrock channels are in a detachment-limited state, in which long-term sediment supply is smaller than transport capacity (e.g., Whipple et al., 2013), is insufficient to account for all observations made in natural streams.

In this paper, I have three separate, yet related aims. First, I develop a description of the mass balance of bedrock channels, based on previous work by Turowski and Hodge (2017) and Turowski (2018). The mass balance is used to derive and discuss the concept of the graded stream for bedrock channels. Second, I derive expressions for response time scales for bedrock channels to adjust to a graded state. Third, ~~For~~ for this~~,~~ it is necessary~~, third,~~ to develop a description of bedrock channel wall erosion by impacting particles. The concepts are used to discuss the current notion of bedrock channels, their possible routes to a graded state and the relevant response time scales.

2 Theoretical considerations

2.1 Mass balance equations for sediment

Landscapes form by the interplay of bedrock erosion, and the entrainment, transport and deposition of sediment, as determined by various drivers such as climate, tectonics, and biological activity. Each erosion process has a minimum of two phases: the break-down of rock mass by chemical or physical weathering, and the entrainment and evacuation of loose pieces of rock that are produced in this way (Gilbert, 1877). From this, it is clear that a minimum description of any eroding landscape needs to include a mass balance equation each for bedrock and for loose sediment. Consider a control volume within a river (Fig. 1), with width W, length L, and a height ranging from the surface, i.e., the interface between bedrock or sediment and the atmosphere, to a fixed reference level somewhere in the bedrock below. The loose material, sediment, overlays the bedrock. Uplift pushes new bedrock into the control volume at a rate T_U, while incision converts it into sediment at a rate I. We assume that the erosion products are small enough so that they are subsequently transported in suspension. Then the rate of change of bedrock mass per unit area M_b is given by:

$$\frac{\partial M_b}{\partial t} = \rho_{\cancel{r}r}(T_U - I)$$

(5)

Here, ρ_r the density of the bedrock. Dividing eq. (5) by ρ_r, and realizing that $h_b = M_b/\rho_r$, we retrieve the usual form of the bedrock mass balance, eq. (4). Details of the derivation of the mass balance for sediment have been given by Turowski and Hodge (2017). Note that working with mass instead of a deposit thickness is advantageous for bedrock channels, because sediment may not be equally distributed on the bed. The entrainment-deposition framework is preferable, because it makes possible to distinguish between moving and stationary sediment, which is necessary to treat the cover and the tools effects. This is not possible when using the Exner approach (Appendix A). The mass balance for the mobile sediment per unit area M_m is given by equation (2)

$$\frac{\partial M_m}{\partial t} = -\frac{\partial q_s}{\partial x} + E - D$$

(6)

The mass balance for the stationary sediment per unit area M_s is given by

$$\frac{\partial M_s}{\partial t} = D - E$$

(7)

Finally, sediment flux q_s and mass M_m are connected via the downstream particle speed U:

$$q_s = UM_m$$

(8)

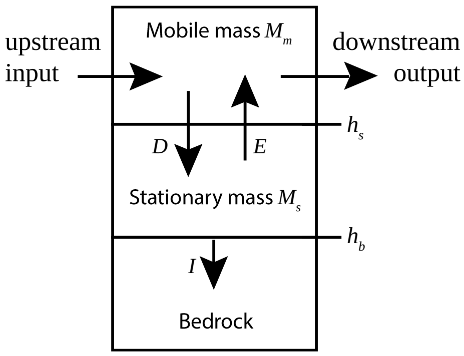

Figure 1: Schematic side view of a control volume within a bedrock channel. The bedrock (bottom) is overlain by stationary sediment (centre), which exchanges particles via entrainment *E* and deposition *D* with the mobile sediment in the water column (top). The bedrock surface h_b lowers at the incision rate *I*, while the sediment surface h_s evolves according to the balance of entrainment and deposition (eq. 6).

2.2 Lateral erosion in bedrock channels by impacting particles

~~T~~Considering impact erosion to be the dominant erosion process, the lateral erosion rate E_L of bedrock channels is driven by particle impacts. ~~and~~ It can therefore, similar to the formulation of the saltation-abrasion model (Sklar and Dietrich, 2004), be written as the product of two terms: (i) the average volume eroded by a single impact, V_i, and (ii) the impact rate per area and time I_r. The latter term can be subdivided into two terms. The first of these quantifies the number of available particles per unit time and area, F_T, which describes the tools effect. The second term F_C describes the effect of bed cover, which captures the effects of the distribution of sediment in the channel on lateral erosion. The need for this term arises because bedload particles generally travel parallel to the channel walls. Sideward deflection is controlled by the interaction of moving particles with the bed (Beer et al., 2017; Fuller et al., 2016), and specifically with stationary sediment, i.e., bed cover (cf. Turowski, 2018).

$$E_L = V_i I_r = V_i F_T F_C$$

(9)

The volume eroded per impact for lateral erosion should be the same as for vertical erosion and has been quantified by Sklar and Dietrich (2004) as the energy of the impact divided by a material constant. It can be evaluated by

$$V_i = \frac{2Y}{k_v \sigma_T^2} \frac{M_p w_i^2}{2}$$

(10)

Here, the first term is related to material properties, where Y and σ_T are Young's modulus of the bedrock and its tensile strength, respectively, and k_v is the rock resistance coefficient. The second term gives the kinetic energy of the impacting grain. Here, M_p is the mass of a single particle and w_i the impact speed normal to the wall.

As in vertical bedrock erosion (Beer and Turowski, 2015; Inoue et al., 2014; Sklar and Dietrich, 2004), the tools effect can be modelled as a linear function of bedload supply Q_s (Mishra et al., 2018), multiplied by a dimensionless factor κ_T with values between 0 and 1 that describes the fraction of bedload available for lateral erosion. To obtain the number of impacting particles per unit area, this product needs to be divided by the mass of a single particle and the total area of the wall A_w that is eroded, to give

$$F_T = \frac{\kappa_T Q_s}{A_w M_p}$$

(11)

Substituting eqs. (10) and (11) into (9), the lateral erosion rate of a bedrock channel can thus be written as

$$E_L = \kappa_T \frac{Y}{k_v \sigma_T^2} \frac{Q_s w_i^2}{A_w} F_{CD}$$

(12)

In eq. (12), there are three parameters that require further discussion: the impact speed w_i, the eroded area A_w and the cover-dependent term F_{CD}. In a previous paper (Turowski, 2018), I argued that lateral erosion and channel width development are intimately related to bed cover. The quantification of all three parameters springs from the physical-conceptual model developed in this previous paper. For this reason the cover-dependent term, F_{CD}, will be discussed first, leading to a quantification of the other two terms, w_i and A_w.

~~**2.2.1 The effect of cover on lateral erosion**~~

In a straight bedrock channel the motion of water and sediment is generally parallel to the walls. Lateral erosion occurs when sediment particles are deflected sideways such that they impact the walls with sufficient force to cause damage. For a given reach, we can define a sideward deflection length scale d, which is relevant for reach-scale lateral erosion (Turowski, 2018). The relevant cross section for setting reach-scale channel width is assumed to be located where the sinuous bedload particle stream crosses from the gravel bar onto the smooth bedrock at the apex of the bar (Fig. 2). Only there, several conditions come together that are favourable to achieve the maximal sideward deflection distances (Turowski, 2018). These are (i) the high particle concentration, (ii) a vector of motion of the particle stream that is already pointing towards the walls, (iii) the existence of roughness necessary for sideward deflection provided by the alluvium, and (iv) the smooth bedrock that does not hinder sideward motion. We expect that the wall is eroded if the uncovered width $W_{uncovered}$ in the cross section is smaller than d (Fig. 3). As a result, we can quantify the cover-dependent term F_{CD} as

$$F_{CD} = \begin{cases} 1 & \text{if} \quad d > W_{uncovered} \\ 0 & \text{otherwise} \end{cases} \tag{13}$$

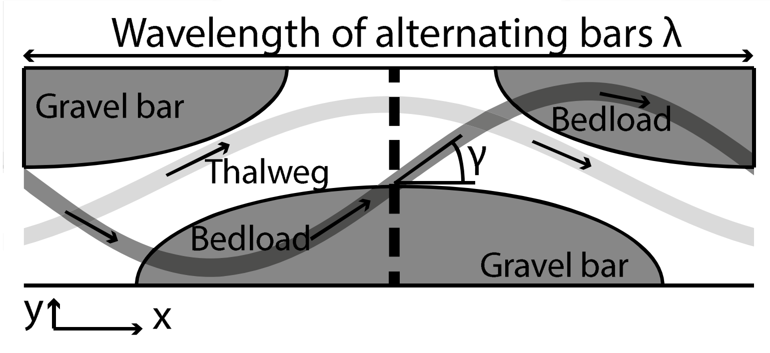

Figure 2: Schematic top view of a straight bedrock channel, with alternating submerged gravel bars (dark grey) on a bedrock bed (white). The sinuous thalweg (light grey) and bedload path (transparent dark grey) are indicated. The black dashed line indicates the cross section that is ideal for sideward deflection of particles; here, the bedload particle stream crosses the boundary between gravel and smooth bedload. The wavelength of the alternating bars and therefore of the bedload path should scale with channel width. Adapted from Turowski (2018).

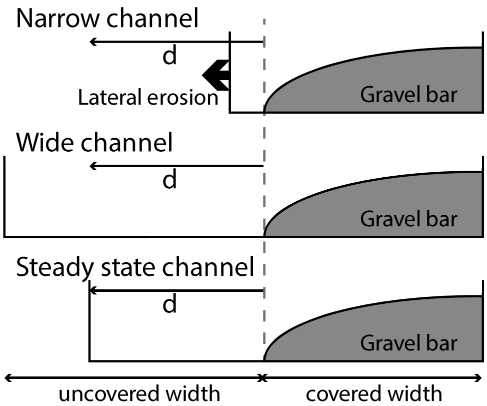

Figure 3: The sideward deflection length scale *d* interacts with bed cover and channel width to determine whether the lateral erosion occurs (top), or not (center, bottom). Adapted from Turowski (2018).

We can write the eroded area on the wall A_w as the product of a length scale and a height. From the argument above, the same particle can attack the wall once when passing each gravel bar. Therefore, the relevant length scale for lateral erosion is the distance between bars on a given side of the channel, i.e., the wavelength of bar spacing, λ. Fuller et al. (2016) observed that for sideward-deflected particles, the erosion height on the wall is larger than the typical saltation hop height. Beer et al. (2017) observed a similar increase in wall erosion rates near boulder obstacles in the channel. When the roughness elements that cause deflection are related to stationary alluvium, we can expect that the height scale is the maximum saltation height of bedload particles at the wall, H_w.

$$A_w = \lambda H_w$$

(14)

Note that not the entire area is eroded at the same time. Rather, particles are deflected towards the wall near the apex of the bars (cf. Turowski, 2018). Consequently, only a small area is eroded at a given time, and the locus of erosion slowly moves downstream as the bars migrate. Likewise, the impact speed w_i and the sideward deflection distance d are related to saltation properties. It is, of course, possible that a particle undergoes several saltation cycles until it impacts the wall. However, in this case, in each additional saltation hop, the sideward component of motion would reduce due to downstream hydraulic forces and frictional loss of momentum. Here, I assume that only during the first hop, particles have sufficient lateral momentum to cause erosion upon impact on the wall. This assumption needs to be verified experimentally.

Since, within the model, sideward deflection is caused by stationary alluvium, particle trajectories should follow those observed for saltation over alluvium (e.g., Abbot and Francis, 1977; Niño et al., 1994), rather than those over bedrock (e.g., Chatanantavet et al., 2013; Auel et al., 2017a). Because the wall-normal component of the motion is relevant for impact erosion (e.g., Sklar and Dietrich, 2004), the particle trajectory needs to be corrected for its angle γ of motion with respect to the wall. Then, the sideward deflection distance d is related to the saltation hop length L_s by

$$d = L_s \sin(\gamma)$$

(15)

Likewise, the impact speed w_i is related to the particle speed U by

$$w_i = U \sin(\gamma)$$

(16)

Auel et al. (2017a) proposed empirical equations to describe saltation properties over a sediment bed as a function of hydraulics, based on their own experiments and a data compilation from various sources. They give the saltation hop length L_s by

$$\frac{L_s}{D} = 1.17\left(\frac{\theta}{\theta_c} - 1\right)$$

(17)

Here, D is grain diameter, θ is the Shields stress and θ_c the critical Shields stress for the onset of bedload motion. Similarly, hop height H_s is given by

$$\frac{H_s}{D} = 0.025\left[\left(\frac{\theta}{\theta_c} - 1\right) + 24\right]$$

(18)

and downstream particle speed U

$$U = 1.46\left[\left(\frac{\rho_s}{\rho} - 1\right) gD\right]^{0.5}\left(\frac{\theta}{\theta_c} - 1\right)^{0.5}$$

(19)

Here, ρ and ρ_s are the densities of the water and sediment, respectively, and g is the acceleration due to gravity. Finally, to close the system of equations, we need some relations describing the geometry of the gravel bars. Alternating bars in bedrock channels have been little studied (e.g., Nelson and Seminara, ~~2011~~2012), and the necessary relations are not available. From a large data compilation of bar width and length in braided channels, Kelly (2006) found that bar length L_{bar} is related to bar width W_{bar} by

$$L_{bar} = 4.95 {W_{bar}}^{0.97}$$

(20)

Based on this observation, I assume that in bedrock channels~~,~~ the wavelength of the bars scales with their width, such that

$$\lambda = \kappa_{bar} W_{bar} = \kappa_{bar} W_{covered}$$

(21)

Here, the bar width has been identified with the covered width $W_{covered}$ (Fig. 2, 3), and κ_{bar} is a dimensionless constant with a value of 2-10, in analogy with bar shapes in alluvial rivers (e.g., Kelly, 2006). Bed cover C is the ratio of covered bed area A_c to total bed area A_{tot}, which can be related to the covered width $W_{covered}$ as follows

$$C = \frac{A_c}{A_{tot}} = \frac{W_{covered}}{W} = \frac{W_{bar}}{W}$$

(22)

Here, W is the channel width. As a result, the bar length can be written as

$$\lambda = \kappa_{bar} W C$$

(23)

Assuming that the maximum saltation height at the wall corresponds to the maximum saltation hop height, $H_w = H_s$, and substituting eqs. (13) to (16), and (18) to (23) into (12), we obtain

$$E_L = \begin{cases} \frac{\kappa Y g}{k_v \sigma_T^2} \left(\frac{\rho_s}{\rho} - 1\right) \sin^2(\gamma) \frac{Q_s}{WC} \frac{\left(\frac{\theta}{\theta_c} - 1\right)}{\left(\frac{\theta}{\theta_c} - 1\right) + 24} & \text{if} \quad d > W_{uncovered} \quad \text{and} \quad \theta > \theta_c \\ 0 & \text{otherwise} \end{cases}$$

(24)

Here, $\kappa = 85\kappa_T / \kappa_{bar}$ is a dimensionless constant. The sideward deflection length scale d can be estimated by the hop length L_s (eq. 24)

$$d = 1.17 D \sin(\gamma) \left(\frac{\theta}{\theta_c} - 1\right)$$

(25)

Finally, the uncovered width can be related to bed cover using eq. (22).

$$W_{uncovered} = W - W_{covered} = W(1 - C)$$

(26)

The rate of change of channel width, in case of a widening channel, should be twice the lateral erosion rate given in eq. (24), since both sides are eroded at the same time.

$$\frac{dW}{dt} = 2E_L$$

(27)

Note that, when $d = W_{uncovered}$, the model gives a stead state channel width consistent with the model of Turowski (2018), with the sideward deflection distance given by eq. (25).

2.3 Timescales of morphological adjustment in bedrock channels

I will now derive analytical expressions for the response time of the channel to perturbations in the boundary conditions, such as changes in discharge, sediment supply or uplift rate. This will be done for three key parameters, channel bed slope, channel width, and cover. For the derivation, it is necessary to assume that, on the time scale of adjustment of one variable, the other variables stay essentially constant. This assumption is reasonable, if a particular variable adjusts much slower than another. For example, slope adjustment takes much longer times than the adjustment of bed cover.

2.3.1 Response time of channel bed slope

Taking the spatial derivative of eq. (4) and assuming spatially constant uplift rate T_U, we obtain

$$\frac{\partial}{\partial x}\frac{\partial h_b}{\partial t} = -\frac{\partial I}{\partial x}$$

(28)

Channel bed slope *S* is defined as the topographic gradient in the downstream direction

$$S = -\frac{\partial h_b}{\partial x}$$

(29)

Equation (28) can thus be rewritten as

$$\frac{\partial I}{\partial x} = -\frac{\partial}{\partial x}\frac{\partial h_b}{\partial t} = -\frac{\partial}{\partial t}\frac{\partial h_b}{\partial x} = \frac{\partial S}{\partial t}$$

(30)

According to the revised saltation-abrasion equation by Auel et al. (2017b), the vertical erosion equation takes the form

$$I = \frac{gY}{230 k_v {\sigma_T}^2}\left(\frac{\rho_s}{\rho} - 1\right)\frac{Q_s}{W}(1 - C)$$

(31)

Steady state cover can be described with the equation by Turowski and Hodge (2017)

$$C = \left(1 - e^{-\frac{Q_s}{M_0 U W}}\right)\frac{Q_s}{Q_t}$$

(32)

The bedload transport capacity can be written as

$$\frac{Q_t}{W} = K_{bl} Q^m S^n$$

(33)

Substituting eqs. (29) to (33) into (28), and assuming that all variables apart from slope are constant, the slope evolution equation takes the form

$$\frac{\partial S}{\partial t} + nBS^{-n-1}\frac{\partial S}{\partial x} = 0$$

(34)

Here, *B* is assumed to be constant.

$$B = \frac{gY}{230 k_v {\sigma_T}^2}\left(\frac{\rho_s}{\rho} - 1\right)\left(1 - e^{-\frac{Q_s}{M_0 W U}}\right)\frac{{Q_s}^2}{K_{bl} W^2 Q^m}$$

(35)

Equation (34) is a non-linear wave equation with celerity c_S

$$c_S = nBS^{-n-1}$$

(36)

The time scale of slope adjustment T_S can therefore be written as

$$T_S = \frac{L}{c_S} = \frac{LS^{n+1}}{nB} = \frac{k_{bl} Q^m L S^{n+1}}{nk\left(1 - e^{-\frac{\overline{q_s}}{M_0 U}}\right){q_s}^2} = \frac{q_t L S}{nk\left(1 - e^{-\frac{\overline{q_s}}{M_0 U}}\right){q_s}^2} = \frac{LSW}{nkQ_s C}$$

(37)

Here, *L* is the length of the reach in question, and *k* is the erodibility, which, according to the revised saltation-abrasion equation by Auel et al. (2017b) takes the form

$$k = \frac{gY}{230 k_v {\sigma_T}^2}\left(\frac{\rho_s}{\rho} - 1\right)$$

(38)

2.3.2 Response time of channel width

For the adjustment of channel width, it is necessary to distinguish between narrowing and widening channels. While channel widening is controlled by the lateral erosion of bedrock walls (see section 2.2, eq. 24), a bedrock channel can only narrow when incising vertically. Therefore, the response time scale of narrowing is related to the vertical incision rate. The timescale of narrowing can be estimated by the time necessary incise the flow depth *H*. After this time, the wetted channel cross-section has been completely replaced. Thus, using the continuity equation (D3) and the expression for flow velocity (D4), the time scale of channel narrowing is

$$T_N = \frac{H}{I} = \frac{(gS)^{\frac{\alpha-1}{2}} R^{\frac{3\alpha-1}{2}}}{k_V I} \left(\frac{Q}{W}\right)^{1-\alpha}$$

(39)

The technique of perturbation analysis can be used to obtain an analytical solution for the width response time in case of a widening channel (e.g., Braun et al., 2015, Turowski and Hodge, 2017). The mathematical details are given in Appendix C, leading to the equation

$$T_W = \frac{18 k_v \sigma_T^2}{\kappa Y \left(\frac{\rho_s}{\rho} - 1\right) g} \frac{\theta_c}{\theta} \frac{W^2}{Q_t} \left(\frac{3}{2C} \frac{Q_s}{M_0 U W} \left(\frac{1}{C} \frac{Q_s}{Q_t} - 1 \right) - \frac{(\alpha - 1)}{C} + (\alpha - 2) \right)^{-1}$$

(40)

Here, M_0 is the minimum mass necessary to cover the bed per unit area, and $\alpha \approx 0.6$ is a dimensionless exponent that appears in the flow velocity equation (see eq. D4; Nitsche et al., 2012). The minimum mass M_0 can be evaluated by assuming that a single layer of closed-packed spherical grains resides on the bed (Turowski, 2009; Turowski and Hodge, 2017)

$$M_0 = \frac{\pi \rho_s D}{3\sqrt{3}}$$

(41)

2.3.3 Response time of bed cover

The response time for the adjustment of bed cover T_C was previously derived by Turowski and Hodge (2017) and is given by

$$T_C = \frac{L M_0 W}{Q_t C}$$

(42)

2.3.4 Response time ratios

The dynamics of the channel during adjustment is to some extent determined by the relative magnitude of the response times. For example, if the response time for the adjustment of bed slope is always much longer than the response time for bed cover, on the time scale of slope adjustment, it can be assumed that bed cover is always at a steady state. The ratio of the response time for slope and width (widening channel) is given by

$$\frac{T_S}{T_W} = \frac{115\kappa}{9n} \frac{SL}{WC} \frac{Q_t}{Q_s} \frac{\theta}{\theta_c} \left(\frac{(\alpha - 1)}{C} - \frac{3}{2C} \frac{Q_s}{M_0 U W} \left(\frac{1}{C} \frac{Q_s}{Q_t} - 1 \right) - (\alpha - 2) \right)$$

(43)

Similarly, for a narrowing channel

$$\frac{T_S}{T_N} = \frac{k_V I L S W}{n k Q_s C} (gS)^{\frac{1-\alpha}{2}} R^{\frac{1-3\alpha}{2}} \left(\frac{Q}{W}\right)^{\alpha-1}$$

(44)

The ratio of the response time for cover and slope is given by

$$\frac{T_C}{T_S} = \frac{gY}{230 k_v {\sigma_T}^2}\left(\frac{\rho_s}{\rho} - 1\right)\frac{nM_0}{S}\frac{Q_s}{Q_t}$$

(45)

The ratio of the response time for cover and width is given by

$$\frac{T_C}{T_W} = \frac{\kappa Y\left(\frac{\rho_s}{\rho} - 1\right) g M_0}{18 k_v \sigma_T^2}\frac{L}{WC}\frac{\theta}{\theta_c}\left(\frac{(\alpha - 1)}{C} - \frac{3}{2C}\frac{Q_s}{M_0 U W}\left(\frac{1}{C}\frac{Q_s}{Q_t} - 1\right) - (\alpha - 2)\right)$$

(46)

Similarly, for a narrowing channel

$$\frac{T_S}{T_N} = \frac{k_V I L M_0 W}{Q_t C}(gS)^{\frac{1-\alpha}{2}} R^{\frac{1-3\alpha}{2}}\left(\frac{Q}{W}\right)^{\alpha - 1}$$

(47)

3 Results

To illustrate the dependence of channel morphology and of the adjustment time scales on control and channel morphology parameters, I used parameter values oriented on Lushui at the Liwu River, Taiwan (Table 1; see Turowski et al., 2007). The values of reach parameters were either measured in the field or estimated using literature data. The value for discharge is representative for bedload-carrying flows, using the partitioning method proposed by Sklar and Dietrich (2006). The value of the exponent and prefactor of the flow velocity equation (D4) was selected using data by Nitsche et al. (2012).

Table 1: Parameter values used for the example calculations, following Turowski et al.'s (2007) estimates for the Liwu River, at Lushui, Taiwan.

Parameter	Symbol	Value
Material properties		
Density of water (kg/m^3)	ρ	1000
Density of sediment (kg/m^3)	ρ_s	2650
Young's modulus (MPa)	Y	5×10^4
Rock tensile strength (MPa)	σ_T	10
Rock resistance coefficient	k_v	10^6
Constants in the equations		
Acceleration due to gravity (m/s^2)	g	9.81
Flow velocity exponent	α	0.6
Flow velocity coefficient	k_V	1
Bedload discharge exponent	m	1
Bedload slope exponent	n	2
Bedload coefficient (kg/m^3)	K_{bl}	11000
Critical Shields stress	θ_c	0.045
Bedload fraction available for lateral erosion	κ_T	0.01
Bar aspect ratio	κ_{bar}	5
Channel reach parameters		
Reach length (km)	L	10
Channel bed slope	S	0.02
Channel width (m)	W	40
Median grain size (m)	D	0.04
Roughness length scale (m)	R	0.2
Water discharge (m^3/s)	Q	~~40~~60
Sediment supply (kg/s)	Q_s	200

3.1 Steady state channel morphology

The sideward deflection length scale d is an important parameter setting channel morphology in steady state, in particular the channel width, which depends on the square root of d (Turowski, 2018).

$$W = \sqrt{\frac{kQ_s d}{I}} = \sqrt{\frac{1.17D\sin(\gamma)\left(\frac{\theta}{\theta_c}-1\right)kQ_s}{I}} \quad (48)$$

Here, d is estimated using saltation hop length of bedload particles over bare bedrock (eq. 25). Saltation hop length is dependent on the Shields stress, and the new formulation can consequently alter steady state scaling of channel width and slope. Unfortunately, equation (48) cannot be solved analytically, since Shields stress θ is non-linearly dependent on channel width and slope (see eq. D6), and a numerical solution is necessary (Fig. 4). As in the model by Turowski (2018), channel width is independent of discharge (Fig. 4A) and the observed scaling between width and discharge arises from a co-dependence of discharge and sediment supply (see Fig. 4B).

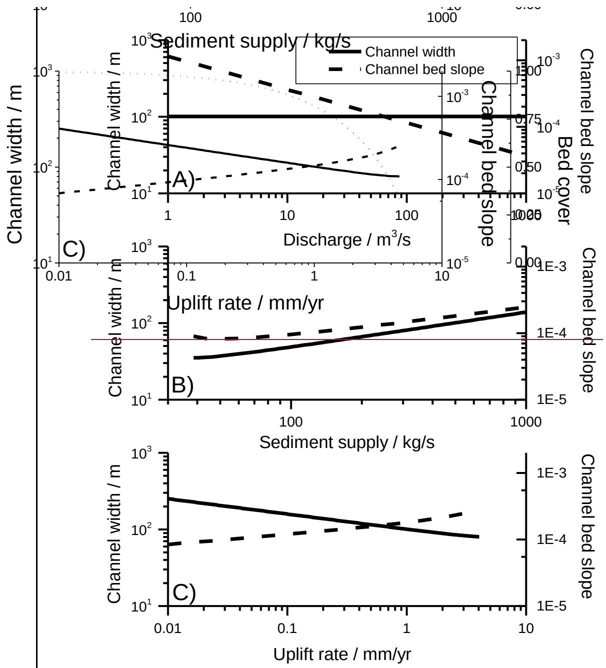

Fig. 4: Steady state channel width (solid line), ~~and~~ channel bed slope (dashed line), and bed cover (dotted line) against forcing variables discharge (A), sediment supply (B), and uplift rate (C). For the calculations, all other parameters have been kept constant (Table 1).

3.2 Controls on adjustment timescales

For the calculation of a~~A~~djustment timescales~~ can be calculated in two separate ways. In the first approach, equations 37, 39, 40 and 41 can be evaluated directly, treating channel width and slope as independent parameters (Fig. 5). For these calculations, I used values for channel width and slope as given in Table 1. For this case, the adjustment time of slope is generally longer than that of width, which is generally longer than that of cover. In the second approach~~, the dependence of width and slope on discharge, sediment supply and uplift rate, and on each other, ~~is ~~needs to be explicitly taken into account. From the derivation (App. C), the relevant width and slope in the time scale equations are those of the steady state morphology corresponding to the relevant control variables. As such, they are not independent of sediment supply, discharge, and other control variables. Within the model, steady state channel width and slope cannot be evaluated analytically, or written in a closed-form equation. Thus, a numerical solution is necessary. ~~In this case, a~~Adjustment time scales of width are generally longer than those for slope and for cover (Fig. ~~6~~5), at least for the parameter values used in the example calculations (Table 1).

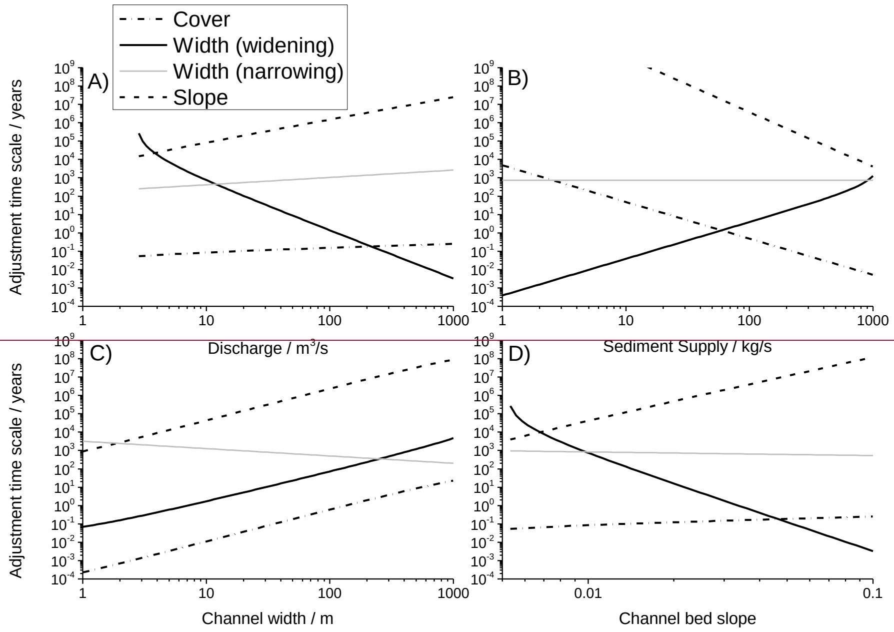

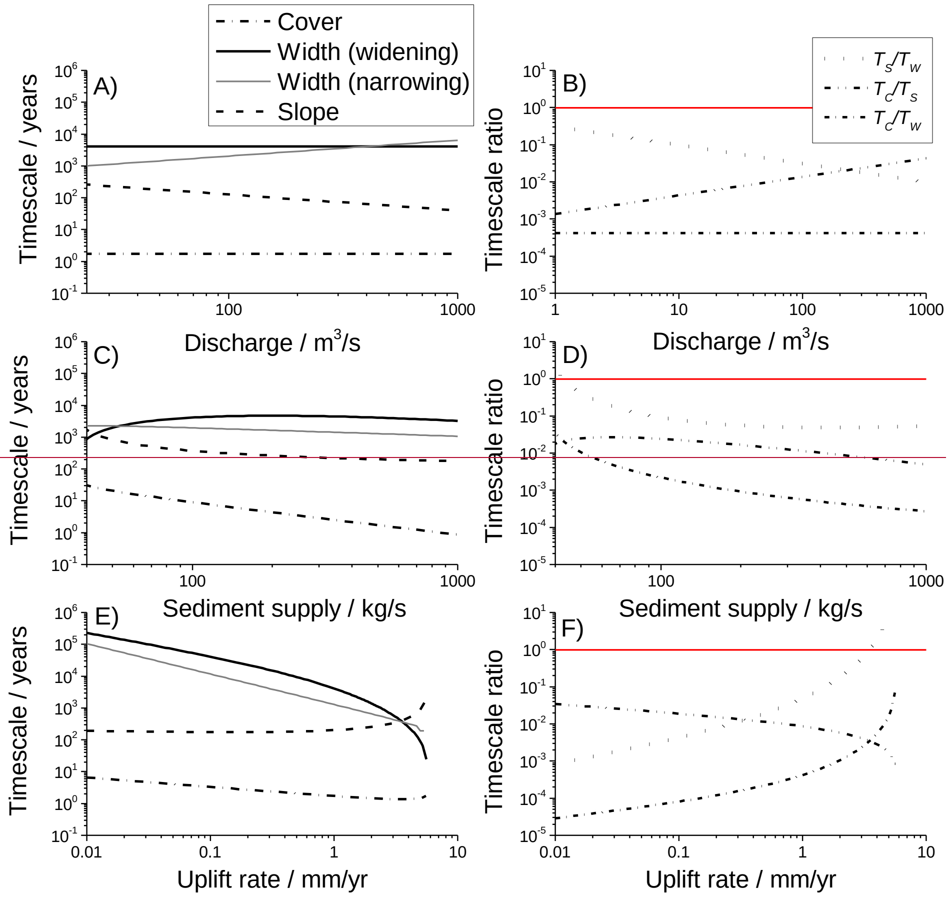

Cover
Width (widening)
Width (narrowing)
Slope
A)
B)
C)
D)
E)
F)
T_S/T_W
T_C/T_S
T_C/T_W
Timescale / years
Timescale ratio
Discharge / m^3/s
Sediment supply / kg/s
Uplift rate / mm/yr

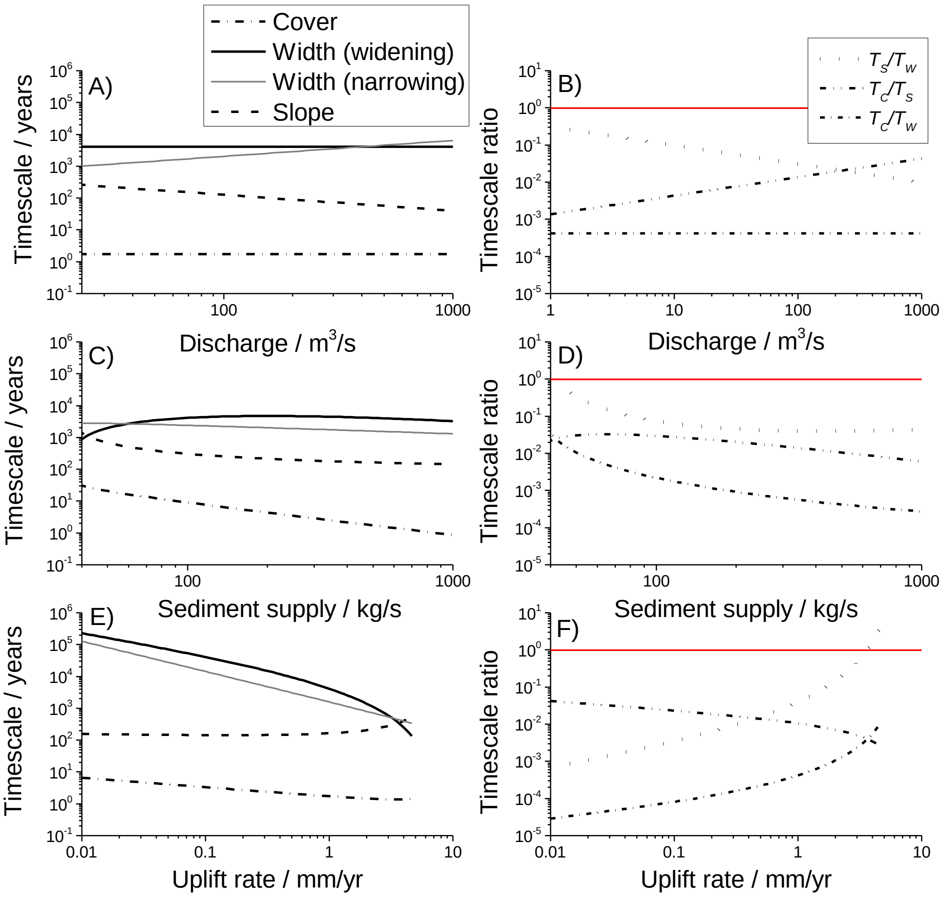

Fig. ~~6~~5: Timescales (left column) and timescale ratios (right column) for channel adjustment, using appropriate steady state values corresponding to imposed discharge, sediment supply and uplift rate, for slope, width and cover, against forcing variables discharge (top row), sediment supply (middle row) and uplift rate (bottom row). For the calculations, all other parameters have been kept constant (Table 1). For the timescale ratios (B, D, F), only the timescale for widening channels was used, due to its similarity with the timescale for narrowing channels (A, C, E). The red solid line in the right column (B, D, F) indicates a ratio of one.

4 Discussion

4.1 Lateral erosion equation

Equation (24) is a mechanistic description of lateral fluvial bedrock erosion by impacting particles. Field and laboratory data that can be used to test the model are scarce, and the few data sets that exist do not include information on all necessary parameters to test it (e.g., Cook et al., 2014; Fuller et al., 2016; Suzuki, 1982; Mishra et al., 2018). The minimum parameters needed for a meaningful test are the lateral erosion rate measured in parallel with relevant driving variables including water discharge and bedload transport rate, in a channel with self-formed sediment cover and alternating gravel bars. Nevertheless, the model provides a starting point for future investigations, providing a clear mechanistic description and a host of testable assumptions and predictions.

Due to lack of direct relevant data and to keep the complexity of the model reasonable, it was necessary to make some assumptions on relevant processes and geomorphic response. For example, bedrock channels at high slopes tend to adjust their bed into a step-pool morphology (Duckson and Duckson, 1995; Scheingross et al., 2019). The feedbacks necessary to develop these bedforms, and how they may affect the flow hydraulics and erosion rates have not been considered in the present model (e.g., Scheingross and Lamb, 2017; Yager et al., 2012). In addition, it was necessary to quantify the wavelength of alternating bars. For the considerations on time scales presented here, the assumption of steady state cover had to be made, implying fully developed bars, and ignoring a potential braiding instability at large channel widths. Nelson and Seminara (2012) provided a linear stability analysis of bar formation over an initially bare bed. They stated explicitly that their considerations to not apply to the geometry of fully formed bars. However, their results and numerical model predictions by Inoue et al. (2016) could be interpreted to suggest that during the transient adjustment to fully formed bars from an initially empty bed under constant forcing conditions, bar wavelength varies little over time. Experimental evidence is rare. Some circumstantial observations can be found in the paper of Chatanantavet and Parker (2008), but these authors do not provide a systematic investigation or conclusive evidence for any type of scaling. In summary, none of the available studies was set up to investigate the controls of fully formed alternating bars, and a full understanding of the controls of their geometry is currently lacking. In absence of a full theory of alternating bars in bedrock channels, I have chosen to keep bar aspect ratio constant (eq. 21) in analogy with observations in alluvial channels (e.g., Kelly, 2006). Yet, due to the coupling with bed cover (eq. 23), this decision leads to unphysical behaviour in the limit of small degrees of cover. In this case, the bar wavelength is small, implying small bar width in comparison to channel width. As a consequence, the meandering bedload path has a large amplitude in comparison to its wavelength, and the deflection angle γ approaches 90°. The assumption about bar wavelength is a minor piece in the model, affecting only the response time channel widening, which is linearly dependent on bar aspect ratio. For a full treatment of bar wavelength, we can speculate on the behaviour in two limits. First, at low values of cover, bar wavelength should be independent of cover, and is likely controlled by channel width or depth. Second, at high cover values, neighbouring bars start to overlap and the relationship to cover likely becomes more complicated. Further theoretical and experimental investigations are necessary to resolve this issue.

The lateral erosion equation (eq. 24) generally aligns with expected relations. Lateral erosion rates increase with increasing shear stress, sediment supply, and erodibility. However, they are inversely proportional to bed cover. This negative relationship arises because gravel bars increase their length as cover increases, due to their constant aspect ratio (eq. 23). This leads to less frequent impacts on the wall by travelling bedload. Fuller et al. (2016) observed that bedrock wall erosion is positively correlated with bed roughness in laboratory experiments. Similarly, Beer et al. (2017) observed higher wall erosion rates next roughness elements in a field study. The data from both of these papers are not sufficient for constraining a functional relationship between roughness and lateral erosion rates. In the model, lateral erosion rate (eq. 24) depends implicitly on roughness, with a positive relationship, via the dependence on shear stress (see eq. D6). A similar implicit dependence can be found for the sideward deflection distance d (eq. 25). Nevertheless, dedicated data on sideward deflection distances are needed to test the current equations and to guide future theoretical developments. Another aspect that is lacking in the current formulation is the dependence of lateral erosion rate on channel curvature. Recent work has attempted to address this within the stream-power framework of bedrock erosion (e.g., Langston and Tucker, 2018; Limaye and Lamb, 2014). Including channel curvature into the present model needs further work on bar deposition and bedload paths within curved channels (cf. Bunte et al., 2006; Fernandez et al., 2019; Mishra et al., 2018; Turowski, 2018).

4.2 Steady state channel morphology

In comparison to the model by Turowski (2018), the sideward deflection length scale *d* has been explicitly quantified in terms of hydraulics (eq. 25), which may alter steady state relationships in comparison to the previously published model. In general, the updated model's predictions align with the results of Turowski (2018). It is somewhat surprising that channel width, like in Turowski's (2018) model, is explicitly independent of discharge (Fig. 4A), and, instead, is set by sediment supply (Fig. 4B). This implies that channel bed slope adjusts to changes in discharge without an effect on channel width, as long as sediment supply stays constant. The results arise~~s~~ because slope and discharge only feature in the same two equations, in that for Shields stress (eq. D6) and that for the bedload transport capacity (eq. C7). Using common parameter values for the relevant exponents *m*, *n* and α, the relationship between slope and discharge is the same in these two equations, allowing the two parameters to co-vary without affecting other parameters. Considering all other parameters constant, the first of these (eq. D6) gives the relation

$$S \sim Q^{\frac{2(\alpha-1)}{\alpha+1}}$$

(49)

while the second one (eq. C7) gives the relation

$$S \sim Q^{-\frac{m}{n}}$$

(50)

With the common parameter choice of α = 0.6 (see Nitsche et al., 2012), *m* = 1, and *n* = 2 (see Turowski, 2018), we find that the two exponents are equal

$$\frac{2(\alpha-1)}{\alpha+1} = -\frac{m}{n} = -\frac{1}{2}$$

(51)

Thus, a change in discharge can be offset by a change in slope, without the need to vary any of the other parameters. Matthematically, this means that by substitution, the number of parameters and equations each can be reduced by one, and slope can be eliminated. A different choice of the *m*/*n* ratio or of α would yield a direct dependence of width on discharge, and a dynamic co-evolution of slope and width.

4.3 Order principles and grade in bedrock channels

The condition of grade can be stated as what I call an order principle, which is a principle after which a dynamic system adjusts state variables to comply with forcing variables. Considering a stream without tributaries or hillslope sediment supply, the order principle for the condition of grade can be stated as follows: A river adjusts such that sediment flux is constant along the stream. The order principle is a direct consequence of the description of the sediment mass balance of the stream (see section 1).

Unlike alluvial channels, which feature a single type of material (the alluvium), in bedrock channels we need to also consider bedrock. This necessitates a second mass balance equation for bedrock (eq. 4), in addition to that for alluvium (see section 2.1). Accepting that a sediment mass balance cannot be neglected for a mechanistic description of bedrock channel dynamics, a bedrock river thus adjusts to two order principles, rather than one. The first of these is related to the mass balance of sediment (section 2.1) and leads to a condition of grade, as discussed above. The second of these is related to the mass balance of bedrock (eq. 4) and can be stated as follows: The river adjusts such that the vertical erosion rate is equal to the uplift or baselevel lowering rate.

When control variables change, the river responds by adjusting its morphology – slope, width, and bed cover – to comply with both of the order principles. However, due to the different adjustment time scales, the path to a new steady state morphology may be complex. As an example, consider a river at steady state, when sediment supply increases. The river responds by depositing sediment, increasing stationary sediment mass (eqs. 6 and 7). The increase in available stationary sediment increases entrainment rates (cf. Turowski and Hodge, 2017). Deposition continues until the river reaches a graded state in which sediment outflux from the considered reach is equal to sediment supply (eqs. 6 and 7). At the same time, any change in stationary sediment directly affects bed cover (eq. 32), and the immediate response of the stationary sediment mass is reflected in the short response times of bed cover (eq. 42; Fig. 5~~, 6~~). Changes in cover, in turn, affect both vertical and lateral incision rates, initiating slope and width adjustment. These adjust much more slowly than bed cover (Fig. 5, 6) until the vertical erosion rate matches the uplift rate. Yet, adjustments in width and slope feed back into the sediment dynamics, for example by affecting transport capacity. Again, the river responds by depositing or entraining material to maintain grade. The mutual feedback continues until both order principles – grade and the erosional balance with matching incision and uplift rates – are satisfied.

With two order principles controlling bedrock channel adjustment, the river may be in a steady state with respect to one of them but not with the other. Because the adjustment time scale for cover is shortest (Fig. 5~~, 6~~), with values that range from minutes to days, it can be expected that bedrock rivers are close to a graded state most of the times (cf. Phillips and Jerolmack, 2016). Given the long adjustment times for width and slope, this does not necessarily mean, however, that they are in a steady state with respect to bedrock elevation, where incision rate matches uplift rate.

4.4 What is a bedrock channel?

The considerations and arguments presented in this paper affect the conceptual view of a bedrock channel, and the use of relevant terminology. We can distinguish detachment-limited and transport-limited channels, which are identified with the two end member descriptions focusing on the mass balance description of bedrock (detachment-limited) and sediment (transport-limited), respectively (cf. Shobe et al., 2017). For detachment-limited channels, we assume that the transport of sediment (eq. 6) can be neglected, i.e., sediment transport does not significantly impact channel dynamics and morphology. Formally, this assumption is valid if sediment supply is very much smaller than transport capacity, or stationary sediment mass $M_s \sim 0$. For transport-limited channels we assume that bedrock incision can be neglected (eq. 4). Formally, this assumption is valid if deposition or erosion has a negligible effect on the stationary sediment mass, in the mathematical limit as M_s goes to infinity. The latter point implies that entrainment or deposition of sediment does not significantly affect stationary sediment mass.

A formal definition of bedrock channels should fulfil a number of criteria (cf. Turowski et al., 2008b). First, the definition should comply with the intuition of field workers. Alluvial and bedrock channels are end members on a continuum of channel types, and therefore, there will always be debated cases. But generally, most geomorphologists would agree whether the particular river is classified as an alluvial or bedrock river when seeing it in the field. Second, it should not rely on observations of field parameters that can change quickly, for example over a single flood. Third, for a classification, a useful definition should not rely on parameters that cannot be measured. Fourth, it should not rely on theoretical concepts that are untested, untestable, or debated. Fifth, a definition rooted in the understanding of relevant processes or dynamics is preferable to one that relies solely on descriptions of morphology.

Bedrock channels, in general, have often been classified as detachment-limited channels, in which long-term sediment-supply is (much) smaller than long-term sediment transport capacity (e.g., Whipple, 2004; Whipple et al., 2013). Further, this condition is generally assumed to result in partial sediment cover and exposed bedrock on channel bed and banks. Bedrock exposure in the channel can easily be observed in the field, and is therefore often used for channel classification (e.g., Montgomery et al., 1996; Tinkler and Wohl, 1998). A number of formal definitions of bedrock channels have been put forward based on these considerations. Exemplary, I will quote and discuss the most recent definition of Whipple et al. (2013):

> *Bedrock rivers may satisfy either or both of the following conditions: (1) the long-term capacity of the river to transport bedload (Qc) exceeds the long-term supply of bedload (Qs), resulting in generally sediment-starved conditions, significant rock exposure in bed and banks, and only thin, patchy, and temporary alluvial cover; or (2) the river is, over the long term (millennial to geologic timescales), actively incising through in-place rock.*

Few geomorphologists would argue against the second part of the definition, although it may difficult to assess this aspect in the field. Nevertheless, it is the first part of the definition that is relevant to the ~~argument~~ points made here, and which I reject based on the following general arguments and on the concepts developed in the present paper. First, the definition is theoretically laden in the sense that a theoretical concept is imposed and equated to a field observation. To my knowledge, no methods currently exist that allow to reliably measure either long-term sediment supply or transport capacity. Even the inaccurate estimates that are currently possible need extensive field and modelling work, partly require strong assumptions, and are subject to large errors (e.g., Schneider et al., 2015). As such, the statement is not useful for the identification of bedrock channels in the field. Second, using mass balance arguments, I have demonstrated that bedrock channels adjust to a graded state. Unlike alluvial rivers, this does not imply that sediment supply is equal to transport capacity. Rather, the relationship between cover and the ratio of supply and capacity is modulated by the deposition and entrainment of stationary sediment mass, i.e., bed cover. The model of Turowski and Hodge (2017) predicts partial cover for sediment supply values larger than transport capacity in some parameter configurations. Similarly, the simulations of Inoue et al. (2016) predict partially covered bed for conditions where sediment supply equals transport capacity. This shows that, depending on the theoretical formulation and the relevant concepts, assumptions, and definitions, sediment supply values equal to or larger than transport capacity may be possible for bedrock channels. Third, even if the long-term sediment supply is lower than transport capacity, alluvial cover is not necessarily thin, patchy or temporary, as is assumed in the definition. Rather, there can be thick, substantial, widespread or persistent cover in the channel. For example, Shepherd (1972) and Fernandez et al. (2019) documented persistent gravel bars in experimental meandering bedrock channels. Theoretical cover models (e.g., Hodge and Hoey, 2012; Sklar and Dietrich, 2004; Turowski and Hodge, 2017) predict substantial cover for certain sediment supply values that are smaller than the transport capacity. Experimental observations of run-away alluviation (e.g., Chatanantavet and Parker, 2008) provide evidence for this. Fourth, in a natural channel, sediment supply and discharge vary over timescales that are short in comparison to the adjustment timescales of channel width and slope. Upscaling discharge variability and sediment supply with a numerical model, Lague (2010) showed that the channel bed is either fully covered or sediment-free for the majority of the time. Long-term mean cover values in his simulations exceeded a value of 0.5 in all cases, prohibiting the use of a detachment- or transport-limited approximation. Taken together, the arguments suggest that the connection between patchy, thin, and temporary alluvial cover and a ratio of sediment supply to transport capacity smaller than one is not tenable. As such, the definition, as proposed, is neither useful nor does it reflect current knowledge of bedrock channel dynamics. Turowski et al. (2008b) proposed an alternative definition, stating that *a bedrock channel cannot substantially widen, lower, or shift its bed without eroding bedrock*. This definition has been discussed and slightly altered by Meshkova et al. (2012). It does not stand in contradiction to field observations, current process knowledge and newly emerged concepts, and can be readily applied in the field (see Turowski et al. 2008b for relevant field criteria).

5. Conclusions

Bedrock channel dynamics are controlled by two dominant order principles. They adjust their morphology both to achieve grade, in which the sediment transport rate is constant along the stream, and to match incision rate to uplift or baselevel lowering. The recognition of a steady state corresponding to one of these principles does not necessarily imply that the other has also been achieved. With minutes to days, the adjustment timescale for bed cover is short relative to the timescales for channel width and slope, and cover may be adjusted to changing supply conditions even over the duration of a single flood event. Thus, it can be expected that bedrock channels are close to a graded state most of the time. In the example calculations (Fig. 5, 6), adjustment timescales for slope and width are of the order of thousands of years. This is shorter than the major cyclic variations of Earth's climate (e.g., Roe, 2006), or the typical timescales of mountain building. The results therefore suggest that many bedrock channels are also close to an erosional steady state, in which erosion rate is equal to uplift rate.

Appendix A: Deriving the Exner equation from the erosion-deposition framework

Substituting eq. (7) into eq. (6) to eliminate entrainment and deposition rates, we obtain

$$\frac{\partial M_m}{\partial t} = -\frac{\partial q_s}{\partial x} - \frac{\partial M_s}{\partial t}$$

(A1)

Rearrange to get

$$\frac{\partial (M_m + M_s)}{\partial t} = -\frac{\partial q_s}{\partial x}$$

(A2)

Define a total sediment mass per unit area $M_{tot} = M_m + M_s$ and divide by the sediment density $\rho_r(1\text{-}p)$ to obtain the Exner equation

$$\frac{1}{\rho_r(1-p)}\frac{\partial M_{tot}}{\partial t} = \frac{\partial h_s}{\partial t} = -\frac{1}{\rho_r(1-p)}\frac{\partial q_s}{\partial x}$$

(A3)

Appendix B: Estimating the deflection angle

Assume that the bedload particle path through the channel follows a sinusoidal path with a wavelength equal to the gravel bar spacing and an amplitude A_{bar}

$$y = A_{bar}\sin\left(2\pi\frac{x}{\lambda}\right)$$

(B1)

Here, y denotes the distance in the cross-channel direction, with the channel centre line located at $y = 0$, and x denotes the distance in the long-channel direction. The tangent of the angle γ is given by the derivative of B1

$$\tan(\gamma) = \frac{dy}{dx} = 2\pi\frac{A_{bar}}{\lambda}\cos\left(2\pi\frac{x}{\lambda}\right)$$

(B2)

We are interested in the deflection angle γ at the edge of the gravel bar, a distance $W_{covered}$, the covered part of the channel width, from the channel boundary, which corresponds to $y = W/2 - W_{covered}$. Hence, at the corresponding x-position x_{edge}

$$2\pi\frac{x_{edge}}{\lambda} = \sin^{-1}\left(\frac{W/_{2} - W_{covered}}{A_{bar}}\right)$$

(B3)

Here, $\sin^{-1}$ denotes the inverse sinus function. Combining equations B1-B3, and writing the path amplitude as a fraction $f = 2A/W$ of the half channel width, we obtain

$$\sin(\gamma) = \sin\left\{\tan^{-1}\left[\pi\frac{fW}{\lambda}\cos\left(\sin^{-1}\left(\frac{1}{f} - \frac{2W_{covered}}{fW}\right)\right)\right]\right\}$$

(B4)

Here, $\tan^{-1}$ denotes the inverse tangent function. Substituting eq. (23) for λ and C for $W_{covered}/W$ (eq. 22), we obtain

$$\sin(\gamma) = \sin\left\{\tan^{-1}\left[\frac{f\pi}{k_{bar}C}\cos\left(\sin^{-1}\left(\frac{1}{f} - \frac{2C}{f}\right)\right)\right]\right\}$$

(B5)

Assuming $f = 1$, a reasonable approximation for the square of B5 (as it appears in all equations) is

$$\sin^2(\gamma) \approx 1 - C$$

(B6)

Appendix C: Deriving the response time scale of width adjustment using perturbation analysis

For the following analysis we assume that all parameters are kept constant apart from sediment supply, which varies sinusoidally over time. This choice allows to obtain an analytical solution for the problem, and does not affect the result for the timescale of transient adjustment. Sediment supply can then be written as the sum of the average supply $\overline{Q_s}$ and a perturbation term δQ_s. The variation of the latter is described with a sinusoidal oscillation around zero.

$$Q_s = \overline{Q_s} + \delta Q_s$$

(C1)

$$\delta Q_s = K \sin\left(\frac{2\pi t}{P}\right)$$

(C2)

Here, K is a constant and P the period of the perturbation. Using linearized approximations to the differential equations (i.e., using first-order Taylor series to approximate non-linear functions), we then derive the width response to this perturbation, which can also be written as the sum of a time-independent term $\overline{W}$ and a time-dependent term δW.

$$W = \overline{W} + \delta W$$

(C3)

To obtain an equation describing the time evolution of channel width, we combine equations (24) and (27) to obtain:

$$\frac{dW}{dt} = \frac{2\kappa Y g}{k_v \sigma_T^2}\left(\frac{\rho_s}{\rho} - 1\right)\sin^2(\gamma)\frac{Q_s}{WC}\frac{\left(\frac{\theta}{\theta_c} - 1\right)}{\left(\frac{\theta}{\theta_c} - 1\right) + 24}$$

(C4)

We substitute the squared sine of the angle by (B6) to obtain

$$\frac{dW}{dt} = \frac{2\kappa Y g}{k_v \sigma_T^2}\left(\frac{\rho_s}{\rho} - 1\right)\frac{1 - C}{C}\frac{Q_s}{W}\frac{\left(\frac{\theta}{\theta_c} - 1\right)}{\left(\frac{\theta}{\theta_c} - 1\right) + 24}$$

(C4)

To simplify the equation further, I make the assumption that excess transport stage θ/θ_c rarely exceeds the value of ten. Then, we can approximate (cf. Auel et al., 2017a):

$$\frac{\left(\frac{\theta}{\theta_c} - 1\right)}{\left(\frac{\theta}{\theta_c} - 1\right) + 24} \approx \frac{1}{36}\frac{\theta}{\theta_c}$$

(C5)

The width evolution equation is then

$$\frac{dW}{dt} = \frac{\kappa Y g}{18 k_v \sigma_T^2}\left(\frac{\rho_s}{\rho} - 1\right)\frac{1 - C}{C}\frac{Q_s}{W}\frac{\theta}{\theta_c}$$

(C6)

Steady state cover can be described with equation (32) (Turowski and Hodge, 2017).

$$C = \left(1 - e^{-\frac{Q_s}{M_0 U W}}\right)\frac{Q_s}{Q_t}$$

(C6)

The bedload transport capacity can be written using eq. (33) (see Turowski, 2018)

$$\frac{Q_t}{W} = K_{bl} Q^m S^n$$

(C7)

$$\frac{dW}{dt} = AK_{bl}Q^m S^n \left(1 - e^{-\frac{Q_s}{M_0 U W}}\right)^{-1} (W)^{\alpha-1} - AQ_s(W)^{\alpha-2}$$

(C8)

With

$$A = \frac{\kappa Y g}{18 k_v \sigma_T^2}\left(\frac{\rho_s}{\rho} - 1\right)\frac{(gS)^{\frac{\alpha+1}{2}} R^{\frac{3\alpha-1}{2}}}{k_V\left(\frac{\rho_s}{\rho} - 1\right) D\theta_c}(Q)^{1-\alpha}$$

(C9)

Here, to reduce the number of parameters and reveal implicit dependencies, the Shields stress has been substituted using standard hydraulic scaling relations (Appendix D). The parameter α is a dimensionless constant that typically takes a value of 0.6, and is a measure of roughness with the dimensions of length (see Nitsche et al., 2012). Next, eqs. C1 and C3 are substituted into C4, and expanded using first-order Taylor approximations of the form

$$(B(\overline{W} + \delta W)^{\alpha-1} - 1) \approx (B\overline{W}^{\alpha-1} - 1) + (\alpha - 1)B\overline{W}^{\alpha-2}\delta W$$

(C10)

$$\left(1 - e^{-\frac{Q_s}{M_0 U W}}\right)^{-1} \approx \left(1 - e^{-\frac{\overline{Q_s}}{M_0 U \overline{W}}}\right)^{-1} - \left(1 - e^{-\frac{\overline{Q_s}}{M_0 U \overline{W}}}\right)^{-2}\left[\frac{1}{M_0 U \overline{W}} e^{-\frac{\overline{Q_s}}{M_0 U \overline{W}}}\delta Q_s + \frac{\overline{Q_s}}{M_0}\left(\frac{1}{U^2 \overline{W}}\frac{\partial U}{\partial W} + \frac{1}{U\overline{W}^2}\right) e^{-\frac{\overline{Q_s}}{M_0 U \overline{W}}}\delta W\right]$$

(C11)

After some algebra and dropping terms that are quadratic or cubic in the delta terms δQ_s and δW, we obtain

$$\begin{aligned}\frac{d\delta W}{dt} = {} & AK_{bl}\left(1 - e^{-\frac{\overline{Q_s}}{M_0 U \overline{W}}}\right)^{-1}(\overline{W})^{\alpha-1} - A\overline{Q_s}(\overline{W})^{\alpha-2} \\ & + \left[AK_{bl}Q^m S^n\left(1 - e^{-\frac{\overline{Q_s}}{M_0 U \overline{W}}}\right)^{-1}(\alpha - 1)\overline{W}^{\alpha-2}\right. \\ & \left. - AK_{bl}Q^m S^n\left(1 - e^{-\frac{\overline{Q_s}}{M_0 U \overline{W}}}\right)^{-2}\frac{\overline{Q_s}}{M_0}\left(\frac{1}{U^2\overline{W}}\frac{\partial U}{\partial W} + \frac{1}{U\overline{W}^2}\right)e^{-\frac{\overline{Q_s}}{M_0 U \overline{W}}}\overline{W}^{\alpha-1} - A(\alpha - 2)\overline{Q_s}\,\overline{W}^{\alpha-3}\right]\delta W \\ & + \left[AK_{bl}Q^m S^n\left(1 - e^{-\frac{\overline{Q_s}}{M_0 U \overline{W}}}\right)^{-2}\frac{1}{M_0 U}e^{-\frac{\overline{Q_s}}{M_0 U \overline{W}}}\overline{W}^{\alpha-2} - A\overline{W}^{\alpha-2}\right]\delta Q_s\end{aligned}$$

(C12)

Resubstituting for cover, particle speed and so on, we obtain

$$\begin{aligned}\frac{d\delta W}{dt} = {} & AK_{bl}\frac{\overline{Q_s}}{\bar{C}Q_t}(\overline{W})^{\alpha-1} - A\overline{Q_s}(\overline{W})^{\alpha-2} + A\overline{Q_s}\,\overline{W}^{\alpha-3}\left[\frac{(\alpha - 1)}{\bar{C}} - \frac{3}{2\bar{C}}\frac{\overline{Q_s}}{M_0 U \overline{W}}\left(\frac{1}{\bar{C}}\frac{\overline{Q_s}}{\overline{Q_t}} - 1\right) - (\alpha - 2)\right]\delta W \\ & + A\overline{W}^{\alpha-2}\left[\frac{\overline{Q_s}}{M_0 U \overline{W}}\left(\frac{1}{\bar{C}}\frac{\overline{Q_s}}{\overline{Q_t}} - 1\right) - 1\right]\delta Q_s\end{aligned}$$

(C13)

Next, equation C2 is substituted in C13 to obtain a differential equation of the form

$$\frac{d\delta W}{dt} = K_1\left[K_2 + K\sin\left\{\frac{2\pi t}{P}\right\} + K_3\delta W\right]$$

(C14)

The general solution to C14 is

$$\delta W = \frac{K_1 K_2\left(\frac{P}{2\pi}\right)}{{K_1}^2{K_3}^2\left(\frac{P}{2\pi}\right)^2 + 1}\sqrt{\left({K_1}^2{K_3}^2\left(\frac{P}{2\pi}\right)^2 + 1\right)}\sin\left\{\frac{2\pi t}{P} + \varphi\right\} + \frac{K{K_1}^2{K_3}^2\left(\frac{P}{2\pi}\right)^2 + K}{{K_1}^2{K_3}^2\left(\frac{P}{2\pi}\right)^2 + 1} + c_1\exp\{K_1 K_3 t\}$$

(C15)

Here, c_1 is the integrative constant and φ is a phase shift of the width response to the perturbation in sediment supply. The exponential term describes transient adjustment to the steady state and can be used to obtain the response time.

$$T_W = -\frac{1}{K_1 K_3}$$

(C16)

Collecting the terms, we obtain

$$T_W = \frac{18 k_v \sigma_T^2}{\kappa Y g} \frac{k_V g D \theta_c}{(gS)^{\frac{\alpha+1}{2}} R^{\frac{3\alpha-1}{2}}} \frac{Q^{\alpha-1}}{\overline{Q_s}} \overline{W}^{3-\alpha} \left(\frac{3}{2\bar{C}} \frac{\overline{Q_s}}{M_0 U \overline{W}} \left(\frac{1}{\bar{C}} \frac{\overline{Q_s}}{Q_t} - 1 \right) - \frac{(\alpha-1)}{\bar{C}} + (\alpha-2) \right)^{-1}$$

(C17)

Equation C17 is considerably simpler in terms of shear stress

$$T_W = \frac{18 k_v \sigma_T^2}{\kappa Y \left(\frac{\rho_s}{\rho} - 1 \right) g} \frac{\theta_c}{\theta} \frac{\overline{W}^2}{Q_t} \left(\frac{3}{2\bar{C}} \frac{\overline{Q_s}}{M_0 U \overline{W}} \left(\frac{1}{\bar{C}} \frac{\overline{Q_s}}{Q_t} - 1 \right) - \frac{(\alpha-1)}{\bar{C}} + (\alpha-2) \right)^{-1}$$

(C18)

In the linear cover approximation (cover-dominated limit; see Turowski, 2018), we have

$$\bar{C} = \frac{\overline{Q_s}}{Q_t}$$

(C19)

Thus, (C18) becomes

$$T_{W,cover} = \frac{18 k_v \sigma_T^2}{\kappa Y \left(\frac{\rho_s}{\rho} - 1 \right) g} \frac{\theta_c}{\theta} \frac{\overline{W}^2}{Q_t} \left(\frac{1}{(\alpha-2) \frac{\overline{Q_s}}{Q_t} - (\alpha-1)} \right)$$

(C20)

Appendix D: Writing shear stress and bedload speed in terms of discharge

The reach-averaged Shields stress θ is defined by

$$\theta = \frac{\tau}{(\rho_s - \rho) g D}$$

(D1)

Here, τ is the shear stress, given by the DuBoys equation

$$\tau = \rho g H S$$

(D2)

The continuity equation for water flow is

$$Q = WHV$$

(D3)

There a number of different equations available to compute water flow velocity V. For mountain streams, a discharge-based variable power flow resistance equation has been found to be a good description of available data (Ferguson, 2007; Nitsche et al., 2012)

$$V = k_V (gS)^{\frac{1-\alpha}{2}} R^{\frac{1-3\alpha}{2}} \left(\frac{Q}{W} \right)^{\alpha}$$

(D4)

Here, R is a measure of bed roughness with dimensions of length, for example the standard deviation of the bed surface (e.g., Nitsche et al., 2012), and $k_V \approx 1$ and $\alpha \approx 0.6$ are constants. Combining C2, C3, and C4, shear stress can be written as

$$\tau = \frac{\rho}{k_V}(gS)^{\frac{\alpha+1}{2}} R^{\frac{3\alpha-1}{2}} \left(\frac{Q}{W}\right)^{1-\alpha}$$

(D5)

The Shields stress is thus given by

$$\theta = \frac{(gS)^{\frac{\alpha+1}{2}} R^{\frac{3\alpha-1}{2}}}{k_V\left(\frac{\rho_s}{\rho}-1\right)gD}\left(\frac{Q}{W}\right)^{1-\alpha}$$

(D6)

The downstream bedload velocity arises in the cover relation (eq. 32), and can be written as:

$$U = 1.46\left(\left(\frac{\rho_s}{\rho}-1\right)gD\right)^{1/2}\left(\frac{\theta}{\theta_c}-1\right)^{1/2}$$

(D7)

In terms of discharge, this evaluates to

$$U = 1.46\left(\left(\frac{\rho_s}{\rho}-1\right)gD\right)^{1/2}\left(\frac{(gS)^{\frac{\alpha+1}{2}} R^{\frac{3\alpha-1}{2}}}{k_V\theta_c\left(\frac{\rho_s}{\rho}-1\right)gD}\left(\frac{Q}{W}\right)^{1-\alpha}-1\right)^{1/2}$$

(D8)

Notation

A_{bar}	Bar amplitude [m].
A_{cover}	Covered bed area [m^2].
A_{tot}	Total bed area [m^2].
A_w	Actively eroding channel wall area [m^2].
a	Scaling exponent, d-A.
B	Constant in non-linear wave equation, describing slope development [m/s].
b	Scaling exponent, β-A.
C	Fraction of covered bed.
C_{SS}	Steady state cover.
c	Scaling exponent, Q-A.
c_s	Celerity of non-linear wave equation, describing slope development [m/s].
d	Sideward deflection length scale, reach [m].
D	Sediment deposition rate per bed area [kg/m^{2}s].
D_{50}	Median grain size [m].
e	Base of the natural logarithm.
E	Sediment entrainment rate per bed area [kg/m^{2}s].
f	Bedload path amplitude as fraction of channel width
F_{CD}	Cover-dependent term in the lateral erosion equation.
F_T	Tools factor in the lateral erosion equation [kg/s].
g	Acceleration due to gravity [m/s^2].
h_b	Bedrock elevation [m].
h_s	Sediment elevation [m].
H	Water depth [m].
I	Vertical erosion rate [m/s].
K_{bl}	Bedload transport efficiency [kg m^{-3m}s^{-m}].
k_e	Erodibility in stream power model [m^{1-3m}s^{1-m}].
k_h	Hydrology coefficient [m^{3-2c}/s].
k_{LE}	Lateral erosion coefficient [m/kg].
k_s	Steepness index [m$^{2\theta}$].
k_{tools}	Lumped constant, tools-dominated channel slope.
k_v	Rock erodibility coefficient.
k_V	Velocity coefficient [m$^{2\alpha}$].
L	Reach length [m].
M_0	Minimum mass per area necessary to cover the bed [kg/m^2].
M_m	Mobile sediment mass [kg/m^2].
M_s	Stationary sediment mass [kg/m^2].
m	Discharge exponent in bedload equation.
m'	Discharge exponent in the stream power model.
n	Slope exponent in bedload equation.
n'	Slope exponent in the stream power model.
q_s	Mass sediment transport rate per unit width [kg/ms].
q_t	Mass sediment transport capacity per unit width [kg/ms].

Q	Water discharge [m^3/s].
Q_c	Critical discharge for the onset of bedload motion [m^3/s].
Q_c^*	Relative sediment supply at the critical cover.
Q_s	Upstream sediment mass supply [kg/s].
Q_s^*	Relative sediment supply; sediment transport rate over transport capacity.
Q_t	Mass sediment transport capacity [kg/s].
R	Bed roughness length scale [m].
S	Channel bed slope.
S_{cover}	Channel bed slope predicted in the cover-dominated approximation.
S_{tools}	Channel bed slope predicted in the tools-dominated approximation.
S_V	Valley slope.
T_C	Time scale of cover adjustment [s].
T_N	Time scale of width adjustment, for a narrowing channel [s].
T_S	Time scale of slope adjustment [s].
T_W	Time scale of width adjustment, for a widening channel [s].
U	Bedload speed [m/s].
V	Water flow velocity [m/s].
W	Channel width [m].
W_{cover}	Covered length within the channel width [m].
$W_{uncover}$	Uncovered length within the channel width [m].
W_{ss}	Steady state channel width [m].
x	Dimensional streamwise spatial coordinate [m].
Y	Young's modulus of the bedrock [kg $m^{-1}s^{-2}$].
α	Scaling exponent, V-Q.
β	Fraction of sediment transported as bedload.
θ	Shields stress.
θ_c	Critical Shields stress for the onset of sediment motion.
λ	Bar wavelength [m].
ρ	Density of water [kg/m^3].
ρ_{bulk}	Bulk density of sediment [kg/m^3].
P_r	Density of bedrock [kg/m^3].
σ_T	Rock tensile strength [kg $m^{-1}s^{-2}$].
κ	Lumped constant, width evolution equation [m^{-2}].
κ_{bar}	Bar aspect ratio.
κ_C	Coefficient in the cover term of width evolution.
κ_T	Coefficient in the tools term of width evolution.
ξ	Average sediment thickness above the bedrock [m].
τ	Bed shear stress [N/m^2].
τ_c	Critical bed shear stress at the onset of bedload motion [N/m^2].

Data availability

No original data were used in this study.

Competing interests

The author declares that he has no conflict of interest.

Acknowledgements

I thank Claire Masteller, Aaron Bufe and Joel Scheingross for discussions. Ron Nativ provided detailed comments on an earlier version of the manuscript.

References

Abbot, J. E., and Francis, J. R. D.: Saltation and suspension trajectories of solid grains in a water stream, Phil. Trans. A, 284, 225-254, 1977.

An, C., Moodie, A. J., Ma, H., Fu, X., Zhang, Y., Naito, K., and Parker, G.: Morphodynamic model of the lower Yellow River: flux or entrainment form for sediment mass conservation? Earth Surf. Dynam., 6, 989-1010, https://doi.org/10.5194/esurf-6-989-2018, 2018.

Auel, C., Albayrak, I., Sumi, T., and Boes, R. M.: Sediment transport in high-speed flows over a fixed bed: 1. Particle dynamics, Earth Surf. Process. Landforms, 42, 1365-1383, https://doi.org/10.1002/esp.4128, 2017a.

Auel, C., Albayrak, I., Sumi, T., and Boes, R. M.: Sediment transport in high-speed flows over a fixed bed: 2. Particle impacts and abrasion prediction, Earth Surf. Process. Landforms, 42, 1384-1396, https://doi.org/10.1002/esp.4132, 2017b.

Beer, A. R., and Turowski, J. M.: Bedload transport controls bedrock erosion under sediment-starved conditions, Earth Surf. Dynam., 3, 291-309, https://doi.org/10.5194/esurf-3-291-2015, 2015.

Beer, A. R., Kirchner, J. W., and Turowski, J. M.: Graffiti for science – erosion painting reveals spatially variable erosivity of sediment-laden flows, Earth Surf. Dynam., 4, 885-894, https://doi.org/10.5194/esurf-4-885-2016, 2016.

Beer, A. R., Turowski, J. M., and Kirchner, J. W.: Spatial patterns of erosion in a bedrock gorge, J. Geophys. Res. Earth Surf., 122, 191–214, https://doi.org/10.1002/2016JF003850, 2017.

Blom, A., Chavarrías, V., and Viparelli, E: The graded alluvial river: Profile concavity and downstream fining, Geophys. Res. Lett., 43, 6285-6293, https://doi.org/10.1002/2016GL068898, 2017.

Braun, J., Voisin, C., Gourlan, A. T., and Chauvel, C.: Erosional response of an actively uplifting mountain belt to cyclic rainfall variations, Earth Surf. Dynam., 3, 1-14, https://doi.org/10.5194/esurf-3-1-2015, 2015.

Bunte, K., Potyondy, J. P., Abt, S. R., and Swingle, K. W.: Path of gravel movement in a coarse stream channel, Proceedings of the Eighth Federal Interagency Sedimentation Conference (8thFISC), 2006, Reno, NV, USA, 162-170, 2006.

Charru, F., Mouilleron, H., and Eiff, O.: Erosion and deposition of particles on a bed sheared by a viscous flow, J. Fluid Mech., 519, 55–80, https://doi.org/10.1017/S0022112004001028, 2004.

Chatanantavet, P., and Parker, G.: Experimental study of bedrock channel alluviation under varied sediment supply and hydraulic conditions, Water Resour. Res., 44, W12446, https://doi.org/10.1029/2007WR006581, 2008.

Chatanantavet, P., Whipple, K. X., Adams, M. A., and Lamb, M. P.: Experimental study on coarse grain saltation dynamics in bedrock channels, J. Geophys. Res. Earth Surf., 118, 1-16, https://doi.org/10.1002/jgrf.20053, 2013.

Chen, A., Darbon, J., and Morel, J.-M.: Landscape evolution models: A review of their fundamental equations, Geomorphology, 219, 68-86, https://dx.doi.org/10.1016/j.geomorph.2014.04.037, 2014.

Church, M.: Bed material transport and the morphology of alluvial river channels, Annual Review of Earth and Planetary Sciences, 34(1), 325-354, https://doi.org/10.1146/annurev.earth.33.092203.122721, 2006.

Cook, K. L., Turowski, J. M., and Hovius, N.: A demonstration of the importance of bedload transport for fluvial bedrock erosion and knickpoint propagation, Earth Surf. Process. Landforms, 38, 683-695, https://doi.org/10.1002/esp.3313, 2013.

Cook, K. L., Turowski, J. M., and Hovius, N.: River gorge eradication by downstream sweep erosion, Nature Geosci., 7, 682-686, https://doi.org/10.1038/ngeo2224, 2014.

Davy, P., and Lague, D.: Fluvial erosion/transport equation of landscape evolution models revisited, J. Geophys. Res., 114, F03007, https://doi.org/10.1029/2008JF001146, 2009.

Duckson, D. W., and Duckson, L. J.: Morphology of bedrock step pool systems, Water Resour. Bull., 31, 43-51, https://doi.org/10.1111/j.1752-1688.1995.tb03362.x, 1995.

Eaton, B. C., and Church M.: A graded stream response relation for bed load–dominated streams, Journal of Geophysical Research: Earth Surface, 109(F3), 2156-2202, https://doi.org/10.1029/2003JF000062, 2004.

Ferguson, R.: Flow resistance equations for gravel- and boulder-bed streams, Water Resour. Res., 43(12), W05427, https://doi.org/10.1029/2006WR005422, 2007.

Fernandez, R., Parker, G., and Stark, C. P.: Experiments on patterns of alluvial cover and bedrock erosion in a meandering channel, Earth Surf. Dynam., in press, https://doi.org/10.5194/esurf-2019-8, 2019.

Fuller, T. K., Gran, K. B., Sklar, L. S., and Paola, C.: Lateral erosion in an experimental bedrock channel: The influence of bed roughness on erosion by bed load impacts, J. Geophys. Res. Earth Surf., 121, 1084–1105, https://doi.org/10.1002/2015JF003728, 2016.

Gilbert, G. K.: Land sculpture. In Geology of the Henry Mountains, Utah, Hunt CB (ed.), Geological Society of America 167. The Geological Society of America: Boulder, CO; 99–150, 1877.

Gleason, C. J.: Hydraulic geometry of natural rivers: A review and future directions, Prog. Phys. Geog., 39, 337-360, https://doi.org/10.1177/0309133314567584, 2015

Heimann, F. U. M., Rickenmann, D., Turowski, J. M., and Kirchner, J. W.: sedFlow – a tool for simulating fractional transport and longitudinal profile evolution in mountain streams, Earth Surf. Dynam., 3, 15-34, https://doi.org/~~doi:~~10.5194/esurf-3-15-2015, 2015.

Hodge, R. A., and Hoey, T. B.: Upscaling from grain-scale processes to alluviation in bedrock channels using a cellular automaton model, J. Geophys. Res. Earth Surf., 117, F01017, https://doi.org/10.1029/2011JF002145, 2012.

Hovius N, and Stark CP.: Landslide-driven erosion and topographic evolution of active mountain belts. In Landslides from Massive Rock Slope Failure, Evans SG, Mugnozza GS, Strom A, Hermanns RL (eds), NATO Science Series IV Earth and Environmental Sciences 49. Springer: Dordrecht; 573–590, https://doi.org/10.1007/978-1-4020-4037-5_30, 2006.

Howard, A. D.: A detachment-limited model of drainage basin evolution, Water Resour. Res., 30, 2261-2285, https://doi.org/10.1029/94WR00757, 1994.

Inoue, T., Izumi, N., Shimizu, Y., and Parker, G.: Interaction among alluvial cover, bed roughness, and incision rate in purely bedrock and alluvial-bedrock channel, J. Geophys. Res., 119, 2123–2146, https://doi.org/10.1002/2014JF003133, 2014.

Inoue, T., Iwasaki, T., Parker, G., Shimizu, Y., Izumi, N., Stark, C. P., and Funaki, J.: Numerical simulation of effects of sediment supply on bedrock channel morphology, J. Hydraul. Eng., 142, 04016014, https://doi.org/10.1061/(ASCE)HY.1943-7900.0001124, 2016.

Johnson, J. P. L., and Whipple, K. X.: Evaluating the controls on shear stress, sediment supply, alluvial cover, and channel morphology on experimental bedrock incision rate, J. Geophys. Res. Earth Surf., 115, F02018, https://doi.org/10.1029/2009JF001335, 2010.

Johnson, J. P. L., Whipple, K. X., and Sklar, L. S.: Contrasting bedrock incision rates from snowmelt and flash floods in the Henry Mountains, Utah, Geol. Soc. Am. Bull., 122, 1600–1615, https://doi.org/10.1130/B30126.1, 2010.

Kelly, S.: Scaling and hierarchy in braided rivers and their deposits: Examples and implications for reservoir modelling, in: Braided rivers: Process, deposits, ecology and management, Sambrook Smith, G. H., Best, J. L., Bristow, C. S., Petts, G. E. (Eds.), Wiley, Chichester, https://doi.org/10.1002/9781444304374.ch4, 2006.

Korup, O., Strom, A. L., and Weidinger, J. T.: fluvial response to large rock-slope failures: Examples from the Himalayas, the Tien Shan, and the Southern Alps in New Zealand, Geomorphology, 78, 3-21, https://doi.org/10.1016/j.geomorph.2006.01.020, 2006.

Lague, D.: Reduction of long-term bedrock incision efficiency by short-term alluvial cover intermittency, J. Geophys. Res., 115, F02011, https://doi.org/10.1029/2008JF001210, 2010.

Langston, A. L., and Tucker, G. E.: Developing and exploring a theory for the lateral erosion of bedrock channels for use in landscape evolution models, Earth Surf. Dynam., 6, 1-27, https://doi.org/10.5194/esurf-6-1-2018, 2018.

Leopold, L. B., and Maddock Jr., T.: The hydraulic geometry of stream channels and some physiographic implications, U.S. Geological Survey Professional Paper, 252, https://doi.org/10.3133/pp252, 1953.

Limaye, A. B. S., and Lamb, M. P.: Numerical simulations of bedrock valley evolution by meandering rivers with variable bank material, J. Geophys. Res. Earth Surf., 119, 927-950, https://doi.org/10.1002/2013JF002997, 2014.

Mackin, J. H.~~ (1948),~~: Concept of the graded river, Geol. Soc. Am. Bull., 59(5), 463-512, https://doi.org/10.1130/0016-7606(1948)59[463:COTGR]2.0.CO;2, 1948.

Meshkova, L. V., Carling, P., and Buffin-Bélanger, T.: Nomenclature, complexity, semi-alluvial channels and sediment-flux-driven bedrock erosion, in Gravel Bed Rivers: Processes, Tools, Environments, Church, M., Biron, P., and Roy, A. (eds). JohnWiley & Sons: Chichester; chapter 31, 424–431, https://doi.org/10.1002/9781119952497.ch31, 2012.

Mishra, J., Inoue, T., Shimizu, Y., Sumner, T., and Nelson, J. M.: Consequences of abrading bed load on vertical and lateral bedrock erosion in a curved experimental channel, J. Geophys. Res., 123, 3147-3161, https://doi.org/10.1029/2017JF004387, 2018.

Montgomery, D. R., Abbe, T. B., Buffington, J. M., Peterson, N. P., Schmidt, K. M., and Stock, J. D.: Distribution of bedrock and alluvial channels in forested mountain drainage basins, Nature, 381, 587-589, https://doi.org/10.1038/381587a0, 1996.

Nelson, P. A., and Seminara, G.: A theoretical framework for the morphodynamics of bedrock channels, Geophys. Res. Lett., 39, L06408, https://doi.org/10.1029/2011GL050806, 2012. ~~Modeling the evolution of bedrock channel shape with erosion from saltating bed load, Geophys. Res. Lett., 38, L17406, https://doi.org/10.1029/2011GL048628, 2011.~~

Niño, Y., García, M., and Ayala, L.: Gravel saltation 1. Experiments, Water Resour. Res., 30(6), 1907-1914, 1994.

Nitsche, M., Rickenmann, D., Kirchner, J. W., Turowski, J. M., and Badoux, A.: Macroroughness and variations in reach-averaged flow resistance in steep mountain streams, Water Resour. Res., 48, W12518, https://doi.org/10.1029/2012WR012091, 2012.

Paola, C., and Voller, V. R.: A generalized Exner equation for sediment mass balance, J. Geophys. Res., 110, F04014, https://doi.org/10.1029/2004JF000274, 2005.

Parker, G.: Hydraulic geometry of active gravel rivers, Journal of the Hydraulics Division, 105, 1185-1201, 1979.

Phillips, C. B. and Jerolmack, D. J.: Self-organization of river channels as a critical filter on climate signals, Science, 352, 694–697, https://doi.org/10.1126/science.aad3348, 2016.

Roe, G.: In defense of Milankovitch, Geophysical Research Letters, 33, L24703, https://doi.org/10.1029/2006GL027817, 2006.

Scheingross, J. S., and Lamb, M. P.: A mechanistic model of waterfall plunge pool erosion into bedrock, J. Geophys. Res., 122, 2079-2104, https://doi.org/10.1002/2017JF004195, 2017.

Scheingross, J. S., Lamb, M. P., and Fuller, B. M.: Self-formed bedrock waterfalls, Nature, 567, 229-233, https://doi.org/10.1038/s41586-019-0991-z, 2019.

Schneider, J. M., Rickenmann, D., Turowski, J. M., Bunte, K., and Kirchner, J. W.: Applicability of bed load transport models for mixed-size sediments in steep streams considering macro-roughness, Water Resour. Res., 51, 5260-5283, https://doi.org/10.1002/2014WR016417, 2015.

Schoch, A., Blöthe, J. H., Hoffmann, T., and Schrott, L.: Multivariate geostatistical modeling of the spatial sediment distribution in a large scale drainage basin, Upper Rhone, Switzerland. Geomorphology, 303, 375-392, https://doi.org/10.1016/j.geomorph.2017.11.026, 2018.

Shepherd, R. G.: Incised river meanders: Evolution in simulated bedrock, Science, 178 (4059), 409-411, https://doi.org/10.1126/science.178.4059.409, 1972.

Shobe, C. M., Tucker, G. E., and Barnhart, K. R.: The SPACE 1.0 model: a Landlab component for 2-D calculation of sediment transport, bedrock erosion, and landscape evolution, Geosci. Model Dev., 10, 4577–4604, https://doi.org/10.5194/gmd-10-4577-2017, 2017.

Sklar, L. S., and Dietrich, W. E.: Sediment and rock strength controls on river incision into bedrock, Geology 29, 1087-1090, https://doi.org/10.1130/0091-7613(2001)029<1087:SARSCO>2.0.CO;2, 2001.

Sklar, L. S., and Dietrich, W. E.: A mechanistic model for river incision into bedrock by saltating bed load, Water Resour. Res., 40, W06301, https://doi.org/10.1029/2003WR002496, 2004.

Sklar, L. S., and Dietrich, W. E.: The role of sediment in controlling steady state bedrock channel slope: Implications of the saltation-abrasion incision model, Geomorphology, 82, 58–83, doi:10.1016/j.geomorph.2005.08.019, 2006.

Stark, C. P., Barbour, J. R., Hayakawa, Y. S., Hattanji, T., Hovius, N., Chen, H., Lin, C.-W., Horng, M.-J., Xu, K.-Q., and Fukahata, Y.: The climatic signature of incised river meanders, Science, 327, 1497-1501, https://doi.org/10.1126/science.1184406, 2010.

Smith, T. R.: A derivation of the hydraulic geometry of steady-state channels from conservation principles and sediment transport laws, The Journal of Geology, 82, 98-104, 1974.

Suzuki, T.: Rate of lateral planation by Iwaki River, Japan, Transactions, Japanese Geomorphological Union, 3(1), 1-24, 1982.

Tinkler, K. J., and Wohl, E. E.: A primer on bedrock channels. In Rivers over rock: Fluvial processes in bedrock channels, Tinkler, K. J., Wohl, E. E. (eds), Geophysical Monograph Series 107, American Geophysical Union: Washington, DC, 1–18, 1998.

Turowski, J. M.: Stochastic modeling of the cover effect and bedrock erosion, Water Resour. Res., 45, W03422, https://doi.org/10.1029/2008WR007262, 2009.

Turowski, J. M.: Alluvial cover controlling the width, slope and sinuosity of bedrock channels, Earth Surf. Dynam., 6, 29-48, https://doi.org/10.5194/esurf-6-29-2018, 2018.

Turowski, J. M., and Cook, K. L.: Field techniques for measuring bedrock erosion and denudation, Earth Surf. Process. Landforms, 42, 109-127, https://doi.org/10.1002/esp.4007, 2017.

Turowski, J. M., and Hodge, R. A.: A probabilistic framework for the cover effect in bedrock erosion, Earth Surf. Dynam., 5, 311-330, https://doi.org/10.5194/esurf-5-311-2017, 2017.

Turowski, J. M., Hovius, N., Hsieh, M.-L., Lague, D., and Chen, M.-C.: Distribution of erosion across bedrock channels, Earth Surf. Process. Landforms, 33, 353-363, https://doi.org/10.1002/esp.1559, 2008a.

Turowski, J. M., Hovius, N., Wilson, A., and Horng, M.-J.: Hydraulic geometry, river sediment and the definition of bedrock channels, Geomorphology, 99, 26–38, https://doi.org/10.1016/j.geomorph.2007.10.001, 2008b.

Turowski, J. M., Lague, D., and Hovius, N.: Cover effect in bedrock abrasion: A new derivation and its implication for the modeling of bedrock channel morphology, J. Geophys. Res. Earth Surf., 112, F04006, https://doi.org/10.1029/2006JF000697, 2007.

Whipple, K. X.: Bedrock rivers and the geomorphology of active orogens, Annu. Rev. Earth Planet. Sci., 32, 151–85, https://doi.org/10.1146/annurev.earth.32.101802.120356, 2004.

Whipple, K. X., Dibiase, R. A., and Crosby, B. T.: Bedrock rivers, in: Treatise on Geomorphology, edited by: Schroder, J. and Wohl, E., Academic Press: San Diego, CA, 550–573, https://doi.org/10.1016/B978-0-12-374739-6.00254-2, 2013.

Whitbread, K., Jansen, J., Bishop, P., and Attal, M.: Substrate, sediment, and slope controls on bedrock channel geometry in postglacial streams, J. Geophys. Res., 120, 779–798, https://doi.org/10.1002/2014JF003295, 2015.

Wickert, A. D., and Schildgen, T. E.: Long-profile evolution of transport-limited gravel-bed rivers, Earth Surface Dynamics, 7, 17-43, https://doi.org/10.5194/esurf-7-17-2019, 2019.

Wobus, C., Whipple, K. X., Kirby, E., Snyder, N., Johnson, J., Spyropolou, K., Crosby, B., and Sheehan, D.: Tectonics from topography: procedures, promise, and pitfalls. In Tectonics, Climate, and Landscape Evolution, Willett, S. D., Hovius, N., Brandon, M. T., Fisher, D. (eds). Geological Society of America Special Paper 398. Geological Society of America: Washington, DC; 55–74, https://doi.org/10.1130/2006.2398(04), 2006.

Tables

Table 1: Parameter values used for the example calculations, following Turowski et al.'s (2007) estimates for the Liwu River, at Lushui, Taiwan.~~Parameter values used for the example calculations.~~

Parameter	**Symbol**	**Value**
Material properties		
Density of water (kg/m^3)	ρ	1000
Density of sediment (kg/m^3)	ρ_s	2650
Young's modulus (MPa)	Y	5×10^4
Rock tensile strength (MPa)	σ_T	10
Rock resistance coefficient	k_v	10^6
Constants in the equations		
Acceleration due to gravity (m/s^2)	g	9.81
Flow velocity exponent	α	0.6
Flow velocity coefficient	k_V	1
Bedload discharge exponent	m	1
Bedload slope exponent	n	2
Bedload coefficient (kg/m^3)	K_{bl}	11000
Critical Shields stress	θ_c	0.045
Bedload fraction available for lateral erosion	κ_T	0.01
Bar aspect ratio	κ_{bar}	5
Channel reach parameters		
Reach length (km)	L	10
Channel bed slope	S	0.02
Channel width (m)	W	~~40~~60
Median grain size (m)	D	0.04
Roughness length scale (m)	R	0.2
Water discharge (m^3/s)	Q	40
Sediment supply (kg/s)	Q_s	200

Figures

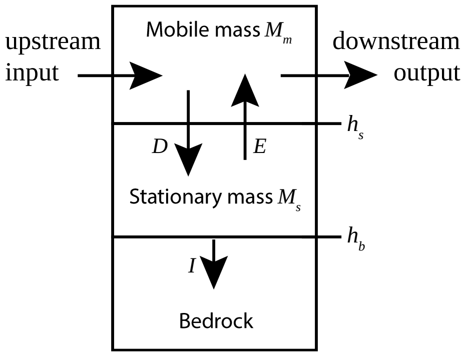

Figure 1: Schematic side view of a control volume within a bedrock channel. The bedrock (bottom) is overlain by stationary sediment (centre), which exchanges particles via entrainment *E* and deposition *D* with the mobile sediment in the water column (top). The bedrock surface h_b lowers at the incision rate *I*, while the sediment surface h_s evolves according to the balance of entrainment and deposition (eq. 6).

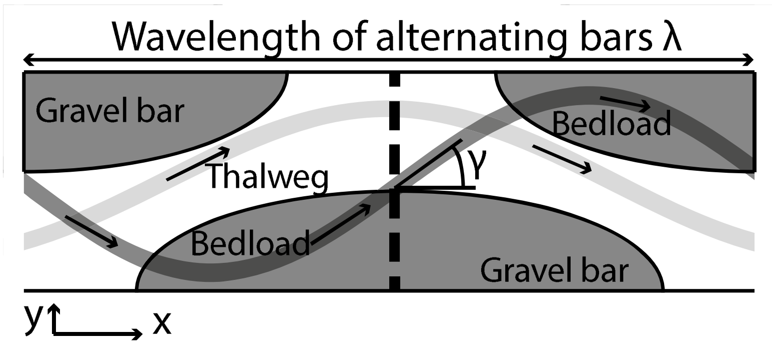

Figure 2: Schematic top view of a straight bedrock channel, with alternating submerged gravel bars (dark grey) on a bedrock bed (white). The sinuous thalweg (light grey) and bedload path (transparent dark grey) are indicated. The black dashed line indicates the cross section that is ideal for sideward deflection of particles; here, the bedload particle stream crosses the boundary between gravel and smooth bedload. The wavelength of the alternating bars and therefore of the bedload path should scale with channel width. Adapted from Turowski (2018).

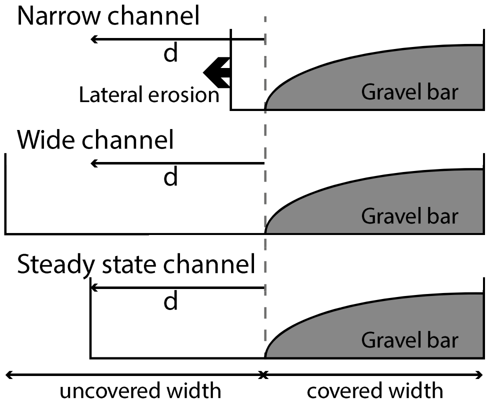

Figure 3: The sideward deflection length scale *d* interacts with bed cover and channel width to determine whether the lateral erosion occurs (top), or not (center, bottom). Adapted from Turowski (2018).

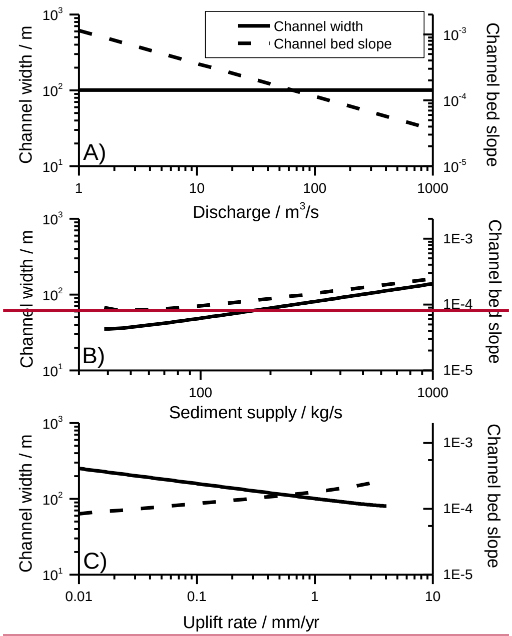

Fig. 4: Steady state channel width (solid line), channel bed slope (dashed line), and bed cover (dotted line) against forcing variables discharge (A), sediment supply (B), and uplift rate (C). For the calculations, all other parameters have been kept constant (Table 1).

~~**Figure 5: Response time scales of cover (eq. 42; dash-dotted line), channel width (eq. 40; black solid line for widening channels,**~~

Fig. ~~6~~5: Timescales (left column) and timescale ratios (right column) for channel adjustment, using appropriate steady state values corresponding to imposed discharge, sediment supply and uplift rate, for slope, width and cover, against forcing variables discharge (top row), sediment supply (middle row) and uplift rate (bottom row). For the calculations, all other parameters have been kept constant (Table 1). For the timescale ratios (B, D, F), only the timescale for widening channels was used, due to its similarity with the timescale for narrowing channels (A, C, E). The red solid line in the right column (B, D, F) indicates a ratio of one.